8-2004

Fractured Branched Circle Packings on the Plane

James Russell Ashe
University of Tennessee, Knoxville

To the Graduate Council:

I am submitting herewith a thesis written by James Russell Ashe entitled "Fractured Branched Circle Packings on the Plane." I have examined the final electronic copy of this thesis for form and content and recommend that it be accepted in partial fulfillment of the requirements for the degree of Master of Science, with a major in Mathematics.

Kenneth Stephenson, Major Professor

We have read this thesis and recommend its acceptance:

Charles Collins, Pavlos Tzermias

Accepted for the Council:
Dixie L. Thompson

Vice Provost and Dean of the Graduate School

(Original signatures are on file with official student records.)

To the Graduate Council:

I am submitting herewith a thesis written by James Russell Ashe entitled “Fractured Branched Circle Packings on the Plane.” I have examined the final electronic copy of this thesis for form and content and recommend that it be accepted in partial fulfillment of the requirements for the degree of Master of Science, with a major in Mathematics.

Kenneth Stephenson
Major Professor

We have read this thesis
and recommend its acceptance:

Charles Collins

Pavlos Tzermias

Accepted for the Council:

Anne Mayhew
Vice Chancellor and
Dean of Graduate Studies

Fractured Branched Circle Packings on the Plane

A Thesis

Presented for the

Masters of Science Degree

The University of Tennessee, Knoxville

James Russell Ashe

August 2004

Acknowledgments

I feel blessed that circumstance has graced me with so many good people. They have been critical in helping me develop into the person that I am. Credit must be given to the department for accepting this ambitious student on the basis of potential rather than background. A possibility I would have never thought possible had it not been for the guidance of Dr. David Dobbs. For the introduction into true math, the beauty it holds, and all the abuse it requires I thank the excellent instruction of Dr. Pavlos Tzermias. The programs used in this thesis were possible because of Dr. Chuck Collins, an expert with Matlab, whose door was never closed and patience never waned. Of course I owe Dr. Kenneth Stephenson for an exciting and elegant problem, but also for his contagious excitement and true love of his area. He gave enough guidance that I was able to achieve my goals, but not enough to rob any thrill of the accomplishment. The discipline and tenacity required in making this difficult journey ascent I owe to my parents and my older brother. My wife was my unsuspecting sherpa, but her commitment and love only strengthened under the pressure. Despite all the added strain that graduate school brings into a marriage she has been the perfect partner. I only hope that I can serve her half as well while she is in vet school. I should also thank Pam Armentrout for her help, advice, excellent references, and candy. There are many other people in the department who deserve recognition. All of the staff has been professional and helpful. All of my instructors have been accessible and excellent teachers. My experience at UT leaves nothing to be desired other then longevity.

Abstract

William Thurston first proposed that real circles could be used to approximate the underlying infinitesimal circles of conformal maps in 1985. Inspired pioneers developed Circle Packing into a very rich and deep field that can be used as a method for constructing discrete conformal maps of surfaces on different types of geometries. Offering the advantages of a computational method that lends itself to experimentation and the easy creation of visual models, Circle Packing has proven itself as valuable new tool in approaching both old and new problems.

In particular, Circle Packing has been used to make discrete analogues of continuous functions; however existing methods are inadequate for certain classical functions. As a solution to this problem, Kenneth Stephenson has suggested using a branched circle packing where the extra angle sum is distributed amongst more than one circle. The purpose of this paper is to investigate the behavior of such circle packings on the plane. The result is the revelation of a subject worthy of interest beyond its potential aide to other problems.

Normally, maps are made in Circle Packing are created by laying out circles adjacently to each other like a group of coins laid out on a table. Taking a group of circles similar to this, we can cut a "slit" from the exterior to a point in the center called the branch point. We can then wrap the cut edges around like a spiraling staircase by a multiple of 2π, creating a branched map. Branched maps are mostly similar to non-branched packings with the exception that they are necessarily globally non-univalent. Adding fractured multiples of 2π to more than a single point does not necessarily result in a map that makes any sense. Regardless of how complicated or simple our original map may be, most of these questions can be answered by surprisingly simple geometry. Furthermore, despite the difficulty that these unfamiliar terms may cause the non-mathematician, the visual nature of circle packing provides models and pictures that bring the concepts to life, making these ideas accessible to most anyone with a high school level understanding of geometry.

Table of Contents

List of Figures

Chapter 1
A Quick Introduction to Circle Packing

Questions involving mutually tangent circles date back to the origins of mathematics and are among some of the most elegant of the classical theorems. Originally, a circle packing might have been described as an arrangement of circles such that each pair of neighboring circles has disjoint interiors and some or all of the circles are (externally) tangent. Such configurations of circles were largely first bridged to analytical functions when William Thurston proposed during a 1985 conference that real circles could be used to approximate the underlying infinitesimal circles in conformal maps and that these approximations would converge to a classical conformal map.[1]

Here we will focus primarily on the Euclidean plane, however circle packings on the hyperbolic plane and the spherical plane are also of great interest to the field. Examples of circle packings on these three geometries can be seen in Figure 1-1. The application of circle packings in the context of discrete conformal maps is the primary source of motivation for study of the field. Although the use of Circle Packing in this realm requires the introduction of more developed definitions and sometimes terse bookkeeping, the grace and beauty of its classical ancestry is preserved in the underlying geometry. I believe that the investigation of our subject is a prime example of this.

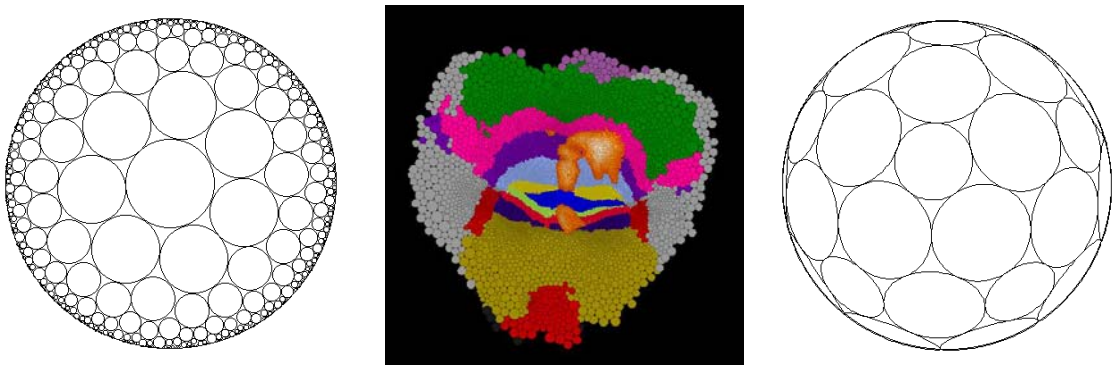

Figure 1-1: Examples of circle packings from left to right on the hyperbolic, Euclidean, and spherical planes.

Source: Monica K. Hurdal, 2004, "Modeling the Brain", [online], http://www.math.fsu.edu/~mhurdal/ (Accessed 7 July 2004).

Definition 1: A *face* is a triangle formed by the centers of three mutually tangent circles. Face $f_0 = \langle v_i, v_j, v_k \rangle$ is the triangle formed from the vertices $v_i, v_j,$ and v_k of their respective circles $c_i, c_j,$ and c_k.

Definition 2: A *Complex* is the tangency pattern for a circle packing. These are encoded as abstract simplicial *2-complexes K*; we assume K is (i.e., triangulates) an oriented topological surface.

Definition 3: A *Circle Packing* , *P*, for a complex, *K*, is a configuration of circles such that for each vertex $v \in K$ there is a corresponding circle c_v, for each edge $\langle v, u \rangle \in K$, the circles c_v and c_u are externally tangent, and for each positively oriented *face* $\langle v, u, w \rangle \in K$ the mutually tangent triple of circles $\langle c_v, c_u, c_w \rangle$ is positively oriented.

Definition 4: A packing is *univalent* if its circles have mutually disjoint interiors. It is *locally univalent* if every circle is mutually disjoint with its externally tangent neighbors.

The complex is just a pattern of tangencies, and this pattern together with the radii of the circles determines the geometry of the packing. A very basic example illustrating this relationship is shown in Figure 1-2. The simplicity of Figure 1-2 belies a central theme of Circle Packing, the special interdependent relationship between a circle packing and its radii. Note that as in Figure 1-3, any three circles can always form a face. However, the situation can be made quite different by adding a single strategically placed circle. Given the complex and the four circles in Figure 1-4, it is clear that no packing exists without manipulating the radii. Fortunately, this can always be done.

Theorem 1: The Monodromy Theorem. Given a complex with associated radii, a necessary and sufficient conditions for existence of a circle packing is that the packing condition be satisfied at every interior vertex (see Theorem 2, pg.8) When this occurs the circle packing is unique up isometries on the plane.

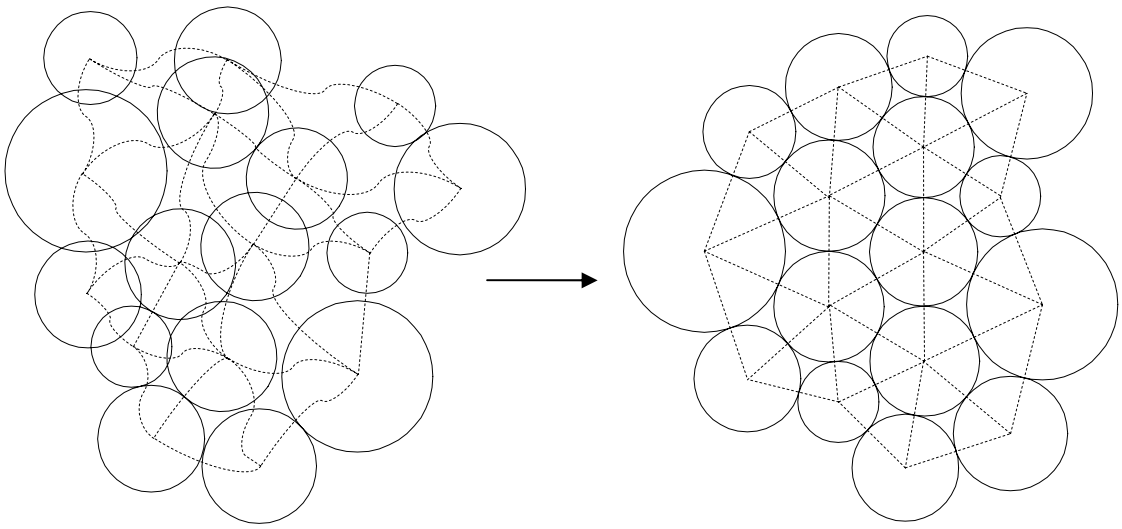

Figure 1-2: A complex with an associated group of radii and the circle packing that they form.

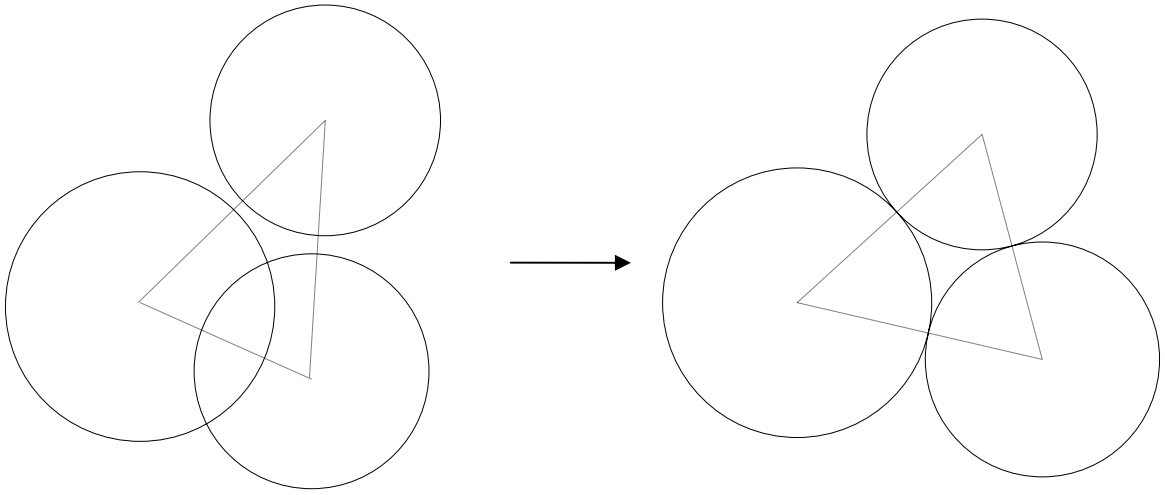

Figure 1-3: Three circles and an associated complex that form a circle packing

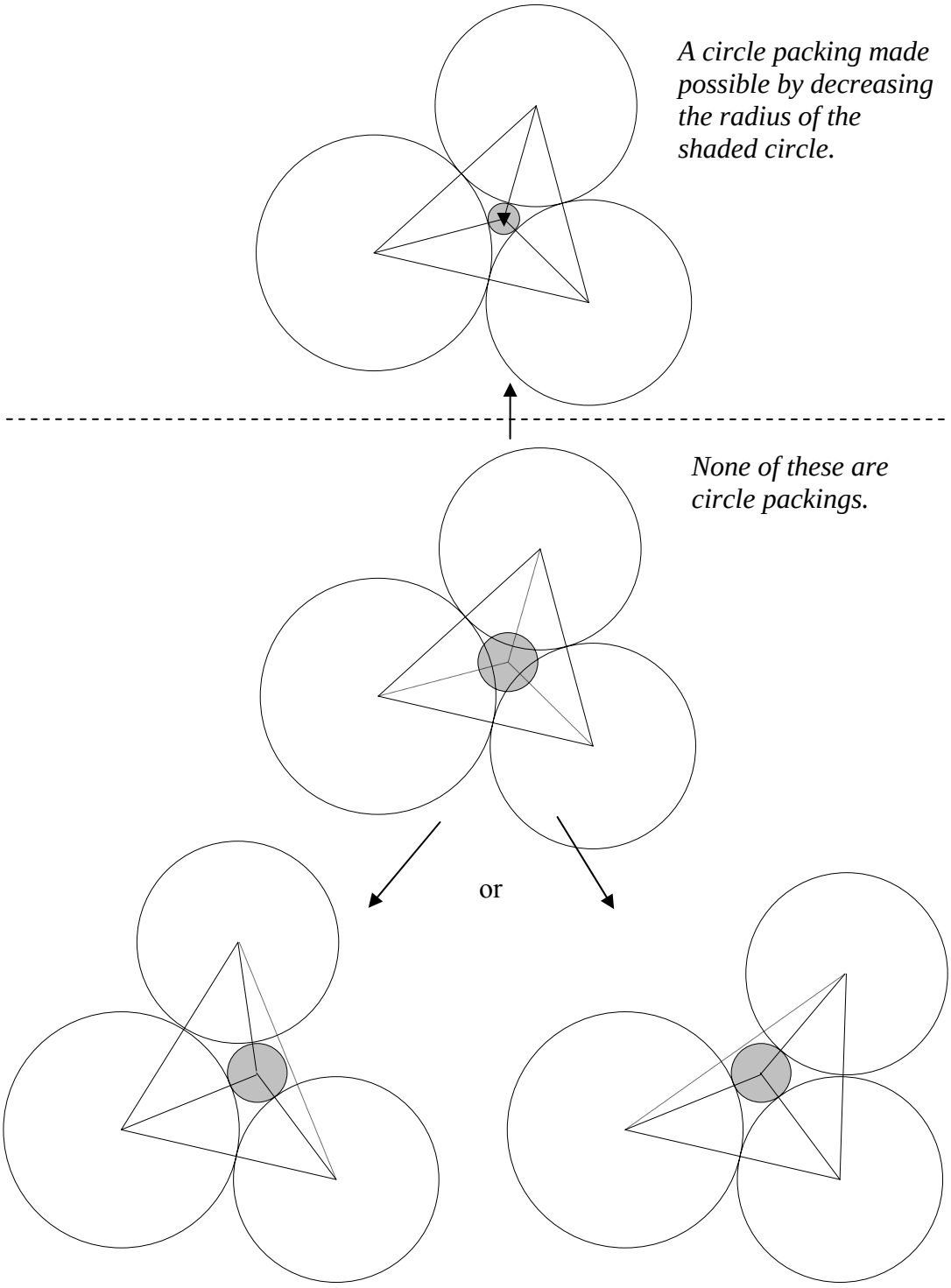

Figure 1-4: The shaded circle has been added to the circle packing from Figure 1-3. The solid lines are use to show circles that are tangent and dashed lines are used to show were tangency has been broken. The complexes of each configuration and radii are identical except for the radius of the shaded circle at the very top

So for any given complex there exists a collection of radii such that a unique circle packing can be formed. The Monodromy theorem has been extended to show that for any finite complex, a unique circle packing will be determined once the radii of the circles on the boundary have been selected.[2] Furthermore we can always compute the radii of the circles for the unique circle packing using the circle packing algorithm developed by Charles Collins and Kenneth Stephenson who have also written an excellent program for making the computations and producing the resulting images.[3]

Figure 1-5 shows a group of "unpacked circles," and the neighboring picture shows the packing after the algorithm has been applied. Once the radii of the interior circles have been determined the resulting packing is unique up to isometries by the Monodromy theorem. As one can see, the relationship between the radii of the circles and their complex in a packing is very rigorous. As illustrated by Figure 1-4, if you make even a small change this relationship will cease to be amenable.

The "non-packings" in Figure 1-4 are three different ways to layout a complex with associated radii that cannot form a circle packing. Such configurations provide a pattern but lack the consistent structure of a circle packing. In our investigation of fractured branched packings distinguishing between complexes and radii that form a packing and ones that do not will be of importance. So we introduce the following definition.

Definition 5: A *motif* is a collection of radii with a complex.

Stated differently, a motif is a complex with associated radii that does not necessarily form a circle packing. So a circle packing is a motif but the converse is not necessarily true. The three different layouts in Figure 1-4 are all representations of the *same* motif. It is an important characteristic of motifs that their layouts will be unique up to isometries if and only if they form a circle packing.

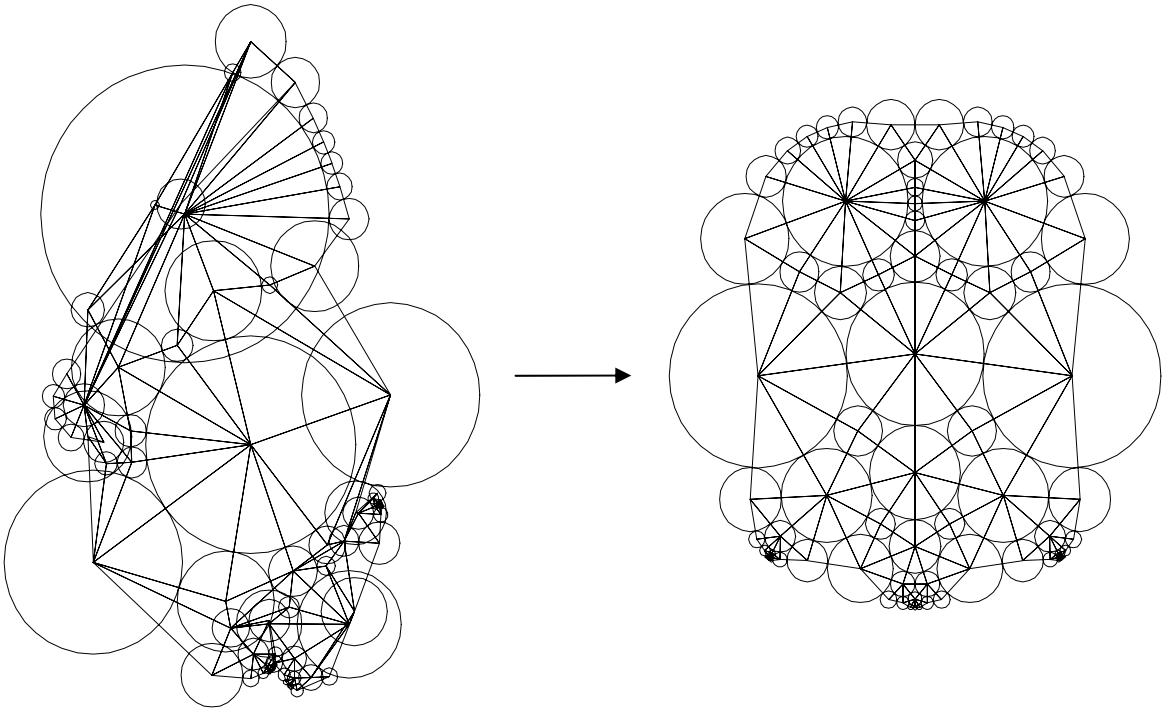

Figure 1-5: The circle packing algorithm in action. This packing is called the *Owl Packing* and has made appearances in many Circle Packing articles.

Chapter 2
Branched Circle Packings

Definition 6: A circle c_v and the circles tangent to it are called a *flower*. The ordered chain, $c_{v_1},...,c_{v_k}$, of tangent circles, called the *petals*, are *closed* when *v* is an interior vertex of the complex formed by all the circles in the flower.

Definition 7: The *angle sum* $\theta(v)$ for vertex *v* is the sum of the angles at c_v in the triangles formed by the triples $\langle c_v, c_{v_i}, c_{v_{i+1}} \rangle$ in its flower.

In the plane, angle sums can be easily computed using the law of cosines, $\theta(v) = \sum_{v,v_i,v_{i+1}} \cos^{-1} = \left(\frac{(r_v + r_{v_i})^2 + (r_v + r_{v_{i+1}})^2 - (r_{v_i} + r_{v_{i+1}})^2}{2(r_v + r_{v_i})(r_v + r_{v_{i+1}})} \right)$ where r_{v_α} is the radius of the circle c_{v_α}. Typically a circle in a circle packing will have an angle sum of 2π. That is, an interior circle's neighbors will wrap around it one complete time.

Definition 8: A *branch circle* in a packing is an interior circle whose angle sum is not 2π. A packing is branched if it has one or more branch circles. The difference of 2π and the angle sum, $b_v = \theta(v) - 2\pi$, is called the branching at C_v, and manipulating the map so that a circle becomes a branch circle is called branching.

Branching a circle packing is not unlike cutting a slit from the boundary to the vertex of the branch circle then wrapping the circle packing around this vertex like a spiraling staircase. For the most part, a circle packing is manipulated by changing its radii. The "wrapping" around a branch circle is caused by changing its radii. If we have some flower, we can increase its angle sum by simply decreasing the radius of the center

circle, c_v. Conversely, the angle sum can be decreased by increasing the radius of the central circle. Refer to Figure 2-1 for an example of a non-branched and branched flower.

Theorem 2: The Packing Condition. The flower of an interior vertex *v* can be realized as a circle packing if and only if $\theta(v) = 2\pi n$ for some integer $n \geq 1$.

A flower with a prescribed complex and radii can only form a packing if it is closed. Therefore a branch circle and its flower form a packing if and only if it meets the packing condition, and a complex with a collection of radii will be a circle packing if and only if the angle sums at all interior circles meet the packing condition. Branching a flower with a non-integer multiple of 2π will result in a motif that is not a packing (see Figure 2-2). We will focus on groups of circles with complexes and radii that immediately fail the packing condition.

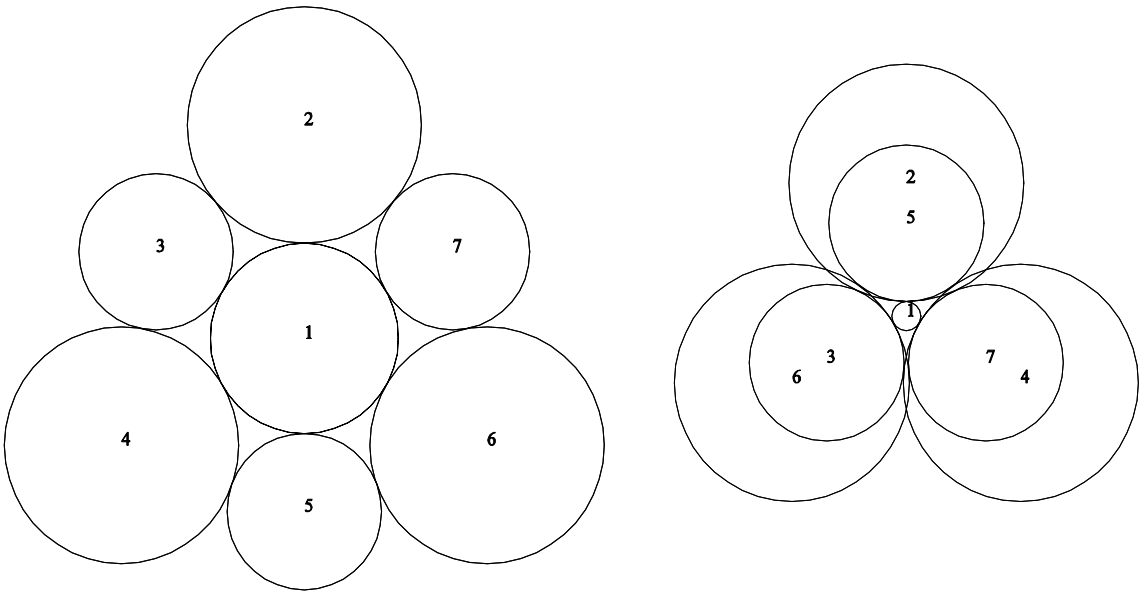

Figure 2-1: On the left is a picture of a flower with a center circle that has an angle sum of 2π. The picture on the right is a branched flower with a center circle (a branch circle) that has an angle sum of 4π. In order to accommodate the extra angle, the center circle has been decreased.

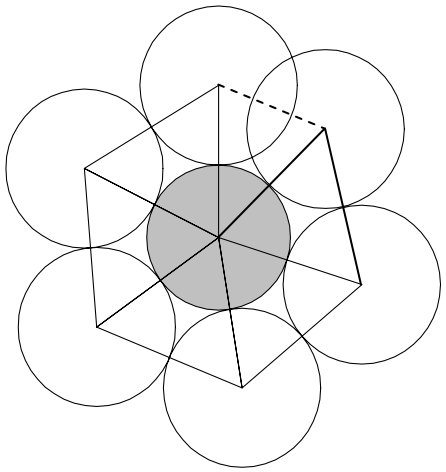

Figure 2-2: The shaded circle has been branched with an angle sum of 2.1π

Chapter 3
Fractured Branched Motifs

Definition 9: A *fractured branched motif* is a motif where *n* interior circles have an angle sum such that $\sum_{1}^{n}\theta(v_i)-2\pi=2\pi$ for $n>1$. The fractured branched motif is non-trivial if $\theta(v_i)>2\pi$ for each branch circle.

We are interested in fractured branched maps manipulated from existing non-branched circle packings. Non-branched circle packings will be branched at more than one circle by decreasing their radii and thus changing their angle sums. Except in the trivial case, fractured branched packings always have at least one circle with an angle sum that does not equal an integer multiple of 2π. Hence by the packing condition, this circle's individual flower will always fail to be a circle packing and so the entire motif will not be a circle packing. Recall from Chapter 1 that motifs which are not circle packings do not have unique layouts. Referring to Figure 1-4 as an example, motifs that are not circle packings lack one of the fundamental qualities that allow Circle Packing to be of service to the study of analytical functions.

However, a fractured branched motif is structured similarly to a circle packing and may retain in part many of the characteristics and behaviors of circle packings. As it turns out, fractured branched motifs can have the rigorous structure of a circle packing by confining where it fails to be circle packing to a localized area of its comlex. These motifs will be like a jigsaw puzzle that properly fits together everywhere except for a few interior pieces. Since we want to minimize the circles that do not "properly fit together" we will fracture the extra angle sum among *mutually tangent interior circles*.

Definition 10: A *coherent packing* is a motif that has a complex and associated radii that meets the conditions for being a circle packing outside a finite interior subset of its complex. Otherwise the motif is an *incoherent packing*.

Given a branched or non-branched motif how do we determine if is coherent or incoherent? This requires some machinery. Recall from Chapter 1 that the layout of a circle packing is independent of the order in which the circles are laid out. By the Monodromy theorem, if we were to take a walk around our packing, beginning with three circles and laying out the rest of the circles in our path according to their complex and radii we would end up in the same place regardless of the path we took.

To determine if a branched motif is a coherent or an incoherent packing we need only take a path that loops around the branched circles. Such a path will travel through flowers that meet the packing condition and avoid the area where it fails. If the loop ends were it began than the motif is a coherent packing. Otherwise we have placed the same circle in two different locations using the same packing criteria and thus the packing is incoherent. With this idea in mind we will proceed formally.

Once a face, say f_1, is placed you can place a neighboring face, say f_2, by simply laying down the single circle that is in f_2 but not in f_1. The faces of the complex rather than its circles can be used as the organizing structure of the motif. This is how we will construct our path around the motif.

Definition 11: A *chain* is a finite sequence of faces $\Gamma = \{f_0, f_1, \ldots f_n\}$ such that each face shares an edge with the preceding face. If all the faces of a chain share a common vertex , *v*, than the chain is called *local* at the vertex *v*. f_0 is called the base face of the chain.

Definition 12: A *closed chain* is a sequence of faces such that the last face and the first face in the sequence share an edge. The class of closed chains Γ, is the set of all closed chains that begin at f_0. $\Gamma_0 = \{f_0\}$ is called the null chain.

Definition 13: A new closed chain Γ' is obtained from Γ by *local modification* if a local subchain of Γ at a vertex, *v*, is replaced by another local subchain at *v* having the same first and last faces.

Definition 14: Two closed chains Γ_1 and Γ_2 are homotopic if one can be obtained from the other from a finite succession of local modifications. See Figure 3-1.

Because a complex is always connected, a chain from one face to any other face in the motif will always exist, and every chain $\Gamma = \{f_0, f_1, \ldots f\}$ will give a unique location for the face, *f*, in a motif. So then the following theorem follows directly from the Monodromy theorem.

Theorem 3: A motif is a packing if and only if the location of a face is independent of the chain used to place it.

Theorem 4: In a circle packing any closed chain is homotopic to the null chain.[4]

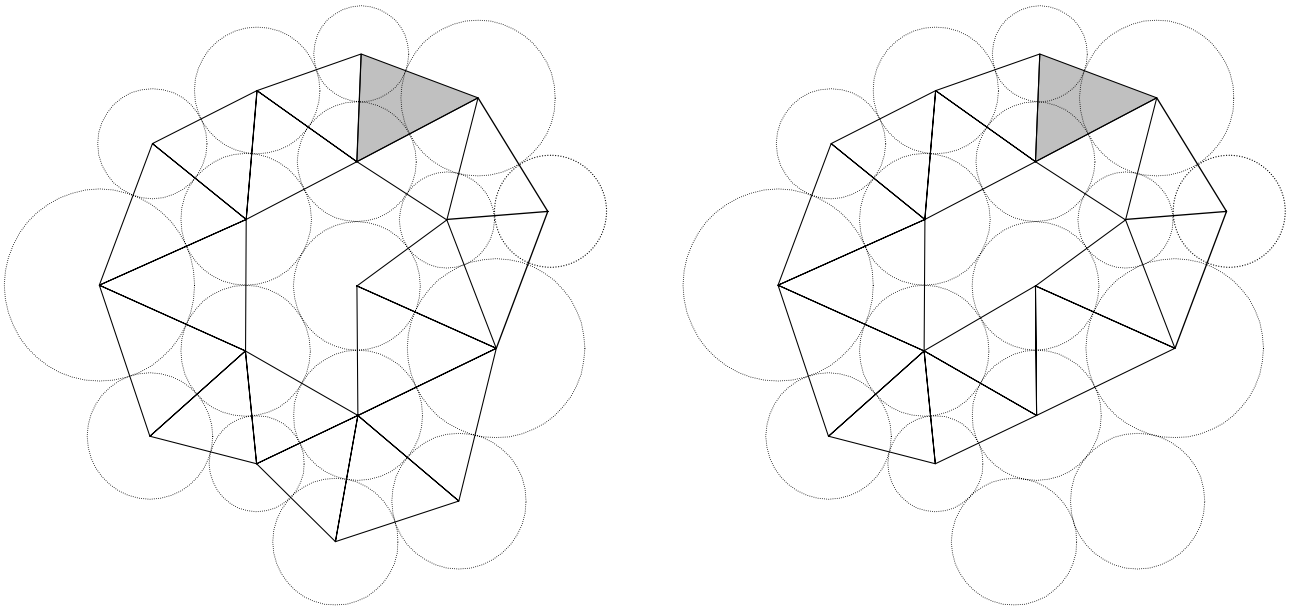

Figure 3-1: Two chains that are null homotopic.

So the location of a face placed by its null chain will only be different from any other chain if the motif is not a circle packing. To check a motif for coherence we need only check that this holds everywhere outside a local area where the packing condition does not hold.

Definition 15: A *holonomy* is a closed chain that forms a single loop around the branch circles and has no face that is composed entirely of vertices of branch circles.

Note that any two holonomies from the same class of closed chains will be homotopic. Every face in a holonomy has at least one vertex that does not belong to a branch circle so then a local subchain that meets the packing condition will be available to make a local modification and we can proceed in making a series of compositions just as if it was a circle packing.

Theorem 5: Developments along homotopic closed chains will place their final face at identical locations if every face of both chains is part of a local chain that meets the packing condition.[5]

Any two holonomies are homotopic, and in fractured branched packings the only flowers that fail to meet the packing condition are those belonging to the branch circles. Hence all homotopic holonomies will place their final face in the same location. So we can check for coherence by comparing the trivial chain of a face to any holonomy from the same class and get the same result.

Choosing a face as a base and constructing a holonomy will result in two triangles. If the Euclidean distance between the vertices of these triangles is zero than the criteria of Theorem 3 is met and the motif is coherent. When the distance is greater than zero the motif is incoherent. This distance is the difference between the locations of the same face laid out with the same method used consecutively, and it can serve as a measure of the level of incoherency.

Theorem 6: A holonomy on a fractured branched packing is a parabolic transformation of its starting face.

Proof. Denote the Euler characteristic of a complex by $\chi(K)$. Note that when a complex triangulates the disc as ours does, $\chi(K)=1$. Let *E* denote the number of edges in *K*, *F* the number of faces in *K*, and *V* the number of vertices in *K*. If E_∂ is the number of edges on the boundary then $E=\frac{3}{2}F+E_\partial$. Which gives, $1=V-(\frac{3}{2}F+\frac{1}{2}E_\partial)+F$ $\Rightarrow 1=V-\frac{1}{2}F-\frac{1}{2}E_\partial \Rightarrow 1=(V_\partial+V_{\text{int}})-\frac{1}{2}F-E_\partial$, where V_∂ is the number of vertices on the boundary and V_{int} is the number of vertices remaining in the interior. The number of vertices on the boundary will equal the number of edges on the boundary, so then $1=V_{\text{int}}-\frac{1}{2}F+\frac{1}{2}V_\partial \Rightarrow 2\pi=2\pi\cdot V_{\text{int}}-\pi F+\pi V_\partial \Rightarrow \pi F=2\pi\cdot V_{\text{int}}+\pi V_\partial-2\pi$. $2\pi\cdot V_{\text{int}}$ is the total of all interior angle sums. By branching we add a total of 2π to this value. Any rotation in the placement of the starting face of a holonomy, f_0, be will determined by the total turning angle of the complex. The total turning interior angle of the non-branched packing is $\pi V_\partial-2\pi$. The number of faces does not change, so then branching changes the total turning interior angle by -2π and the total exterior turning angle will be 2π. Thus a holonomy results in no turning (modulo 2π), no scaling, because the radii do not change, and hence it must be a translation, i.e. the holonomy is parabolic

Because the transformation is parabolic, there will be no ambiguity when measuring the distance between where the holonomy lays its first and last face. If we begin with a circle packing as in Figure 3-2, adjust the angle sums of three interior circles by distributing a total of an extra 2π among them, and then apply the circle packing algorithm then we will have a fractured branched motif as in Figure 3-3. Now using this

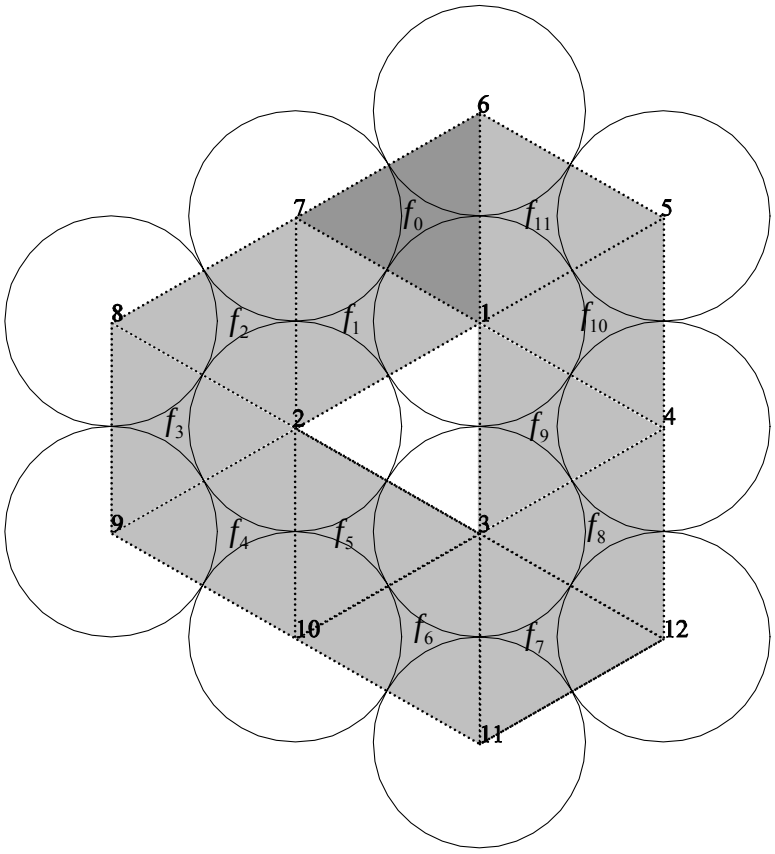

Figure 3-2: The twelve labeled circles form a circle packing. The shaded faces form the closed chain, $\Gamma = \{f_0, f_1, f_2, f_3, f_4, f_5, f_6, f_7, f_8, f_{10}, f_{11}\}$.

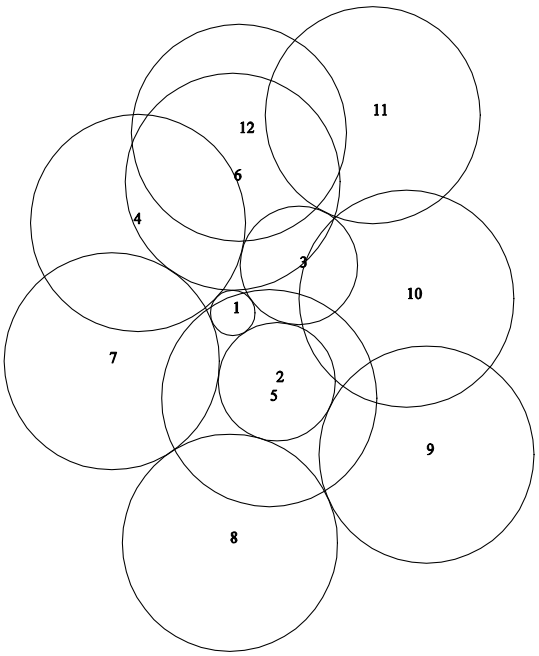

Figure 3-3: A fractured branched motif that was created by adding $\frac{3}{2}\pi$ to circle 1, $\frac{1}{4}\pi$ to circle 2, and $\frac{1}{4}\pi$ circle 3.

fractured branched motif, a holonomy that encircles the branch circles can be used to test for coherency. If the motif is incoherent then the first face of the holonomy will be a parabolic shift as in Figure 3-4. Repeatedly laying down the faces of the holonomy will result in repetitive parabolic shifts. In Figure 3-5 the same holonomy has been followed through five times.

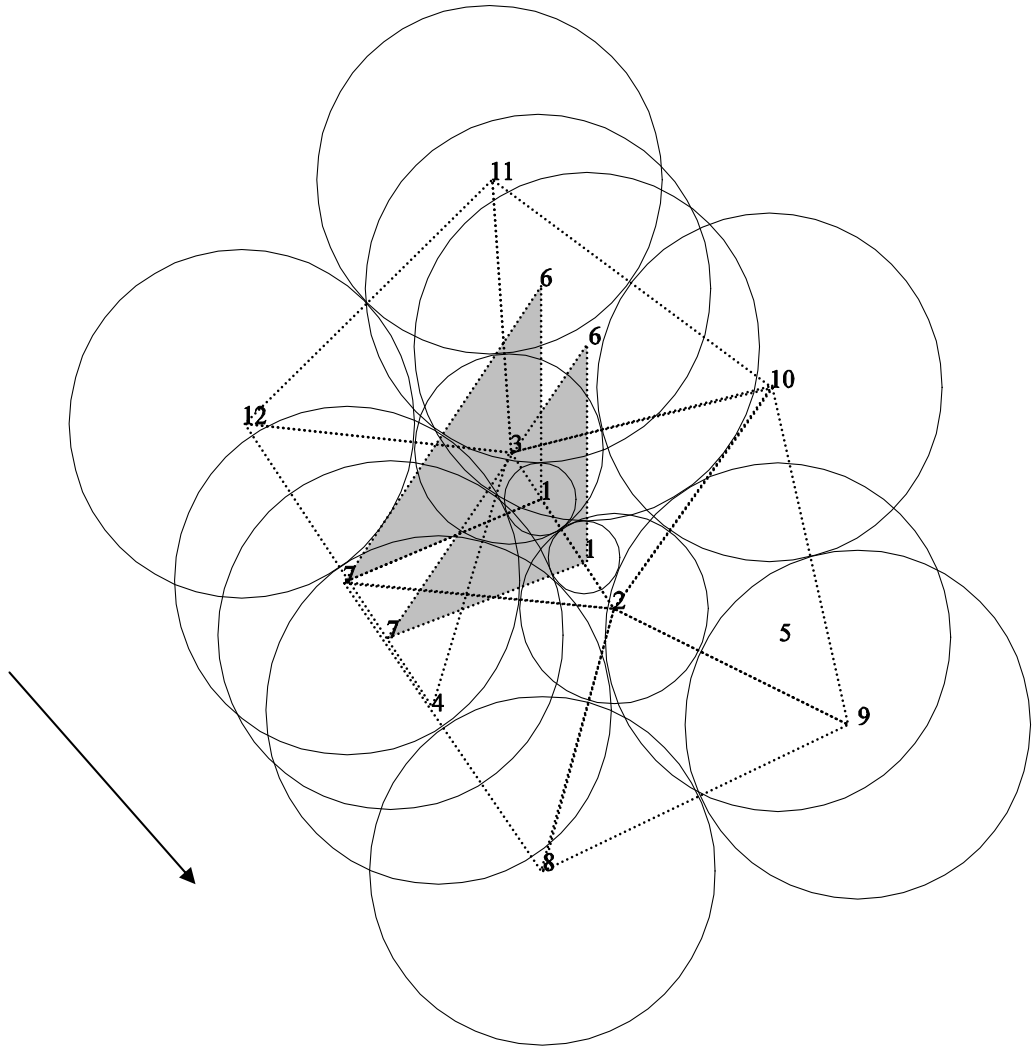

Figure 3-4: Laying down the faces in the closed chain illustrated in Figure 3-2, a holonomy is constructed. The shaded face, f_0, is the first face of the chain and placed in two different locations. Clearly, this motif is incoherent.

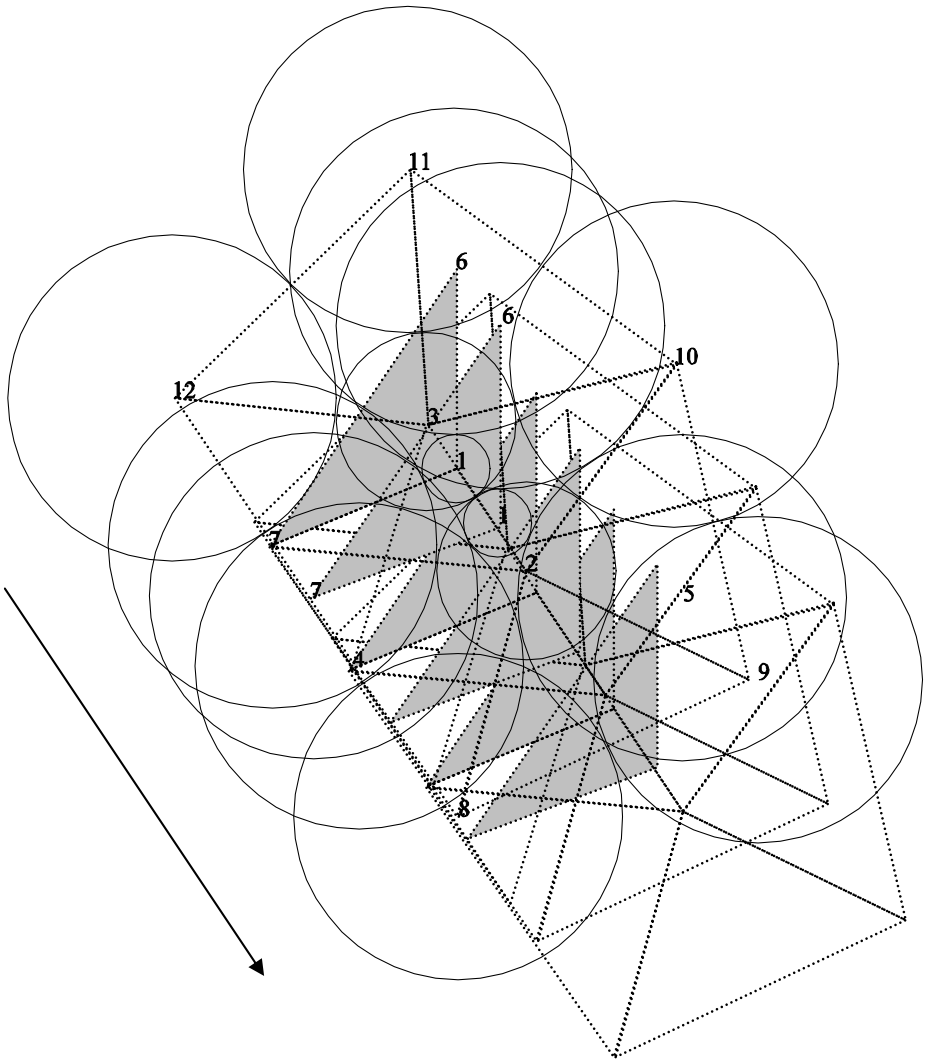

Figure 3-5: The holonomy from Figure 3-2 has been laid out repeatedly.

Chapter 4

Experiments with Fractured Branched Motifs

One of the great advantages of Circle Packing is its computability. Together with the existence of programs to do the computation, Circle Packing lends itself to high level experimentation. Experiments using fractured branch motifs with two, three, and four branch circles are presented. Experiments were conducted with a variety of "typical" and "atypical" packings, however they all had very similar results so we will repeatedly use the same packing. Here we start with the non-branched basic packing shown in Figure 4-1. The holonomy used to measure incoherency is also shown.

Experiments with Two Branch Points

The sum of the branching added is always 2π. In Figure 4-2 the x-axis scales 0-1 for the portion of this 2π that has been placed on circle 1. The remaining extra angle sum is necessarily placed on circle 2. The y-axis measures the parabolic distance that the holonomy has moved the base triangle.

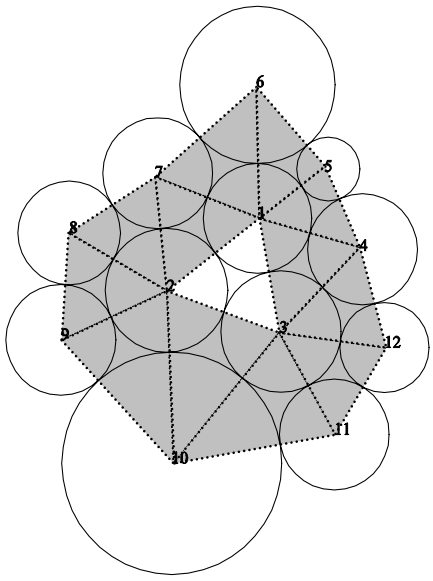

Figure 4-1: The circle packing used in the 2 and 3 branch circle experiments. The holonomy that is used is shaded.

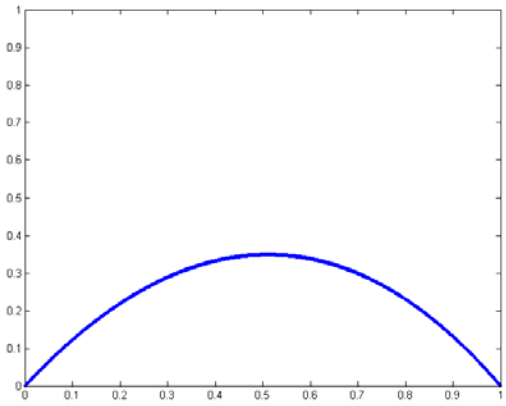

Figure 4-2: 3000 random distributions of the branching distributed between two circles.

As this graph suggests, there is in fact no non-trivial fractured branching distribution with two branch circles that will result in a coherent packing. This will be shown in the (next) section.

As should be expected, a small change from a trivial branching where we know the motif is a packing causes only a small amount of misplacement. The shape of these circles could change if the radii of the border circles were to change. Particularly it seems to be the ratio of the border circles' radii that is the determining force. Figure 4-3 is the same experiment that was conducted with Figure 4-2. The complex of this packing is identical to the one above; only the radii of circles 2 and 7 have been made very large. The distribution that yields the maximum parabolic shift for the base face has moved noticeably towards the left.

As we will see later, the placement of the circles tangent to a border circle occurs directly as a result of the branch circle's radii. In non-fractured branched motifs this immediately translates into a change of angle sums. Fractured branched motifs have their angle sum changed by their own radius and radii change occurring as a result of branching at other circles. This relationship is demonstrated in part by the behavior of these parabolas. A further study of how radii distribution effects their shape may lead to a better solution for finding a coherent fracturing than the one presented in Chapter 6.

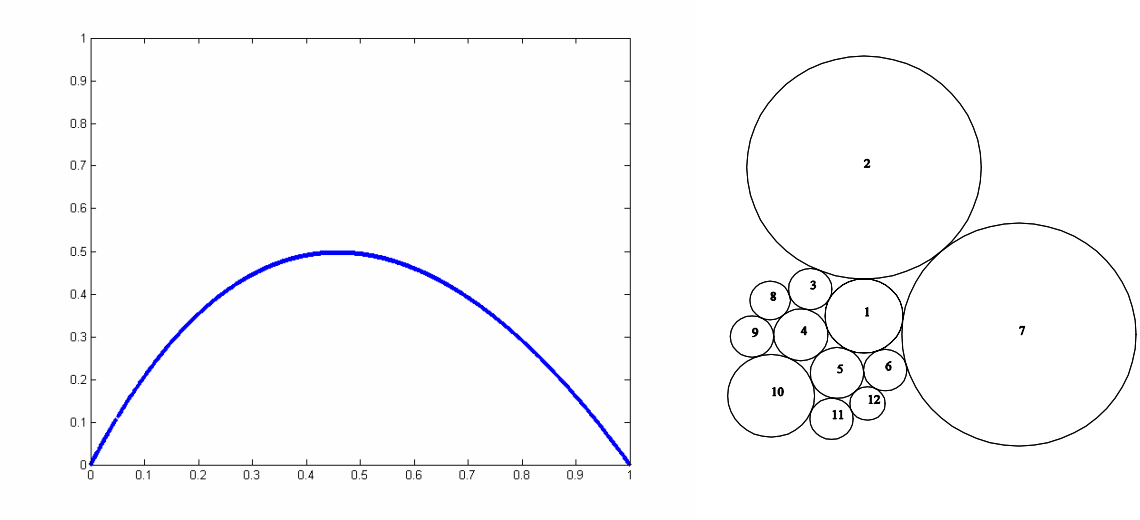

Figure 4-3: On left is a graph of 3000 experiments of the branching distributed between two circles. On the right is a picture of the packing used.

Experiments with Three Branch Circles

This next experiment is shown in Figure 4-4. It is the most interesting in this chapter, and since we are focusing on motifs with three branch circles it is also the most relevant. The distribution is always a partition of 2π so this can be drawn in $\mathbb{R}^3$. The x-axis is the percentage of branching at circle 1, the y-axis is the percentage at circle 2, and the z-axis is the resulting translation distance of the holonomy.

These incoherent maps certainly do behave nicely! Just as in the case of two branch circles the error grows as the distribution moves away from the trivial solutions. These graphs suggest two glaringly obvious properties. First, there appears to a single interior point with a height of zero, meaning that a non-trivial coherent distribution exists. Second, that this distribution is unique. The smooth continuous shape also suggests that an iterative process would converge to that unique solution. We will show that all of these conjectures are true for a special case.

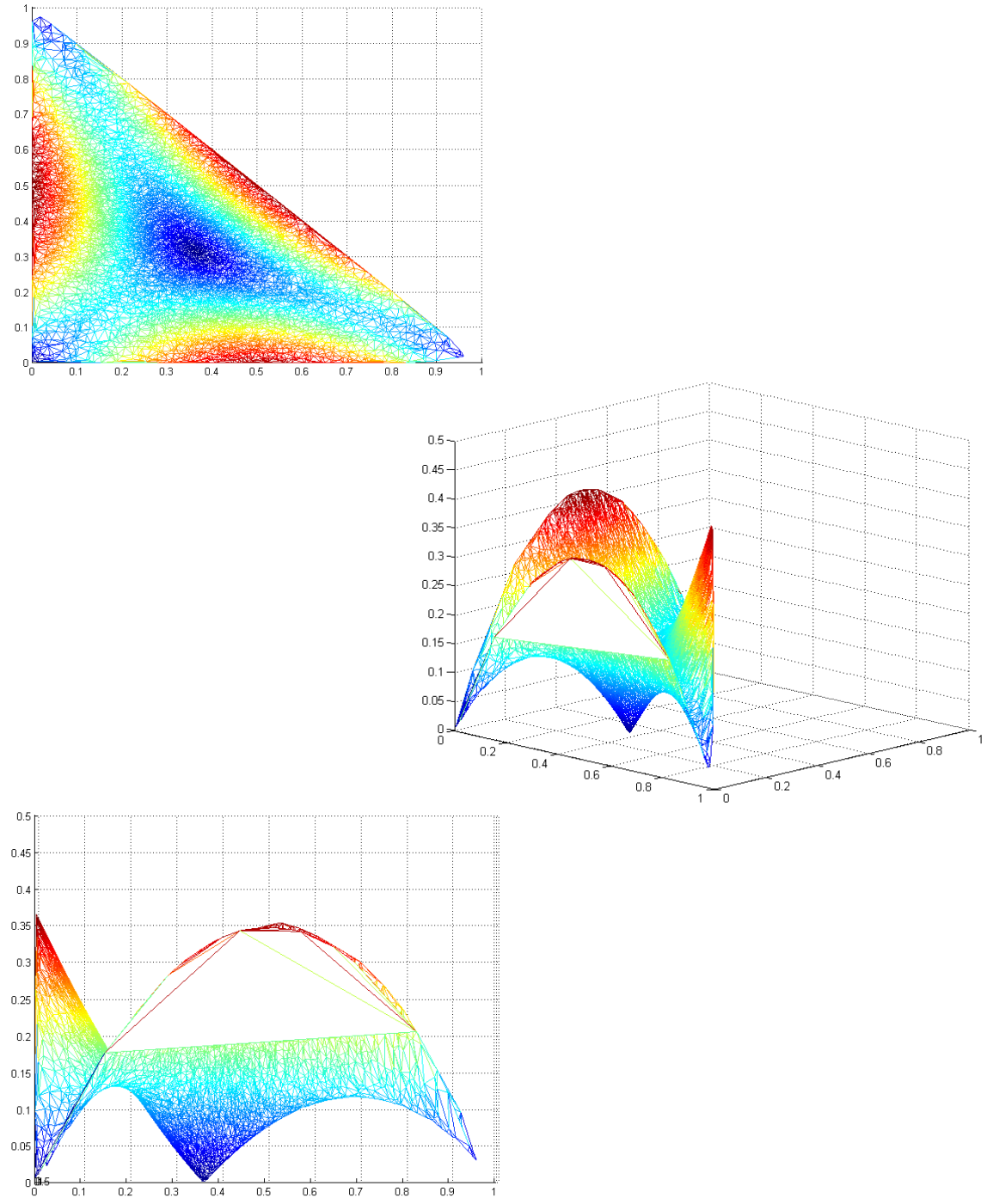

Figure 4-4: 10,000 experiments of the branching distributed between three circles. From top to bottom is a top, angled, and side view.

Experiments with Four Branch Circles

The experiments with three branch circles may bring interest in the geometric structure of these types of fractured motifs, but the uniqueness characteristic means that they will probably not be applicable in approximating analytical functions because they would lack the necessary flexibility. Apparently, it will be necessary to attempt using four branch circles. This paper will focus on the case with three branch circles, but a few experiments could give direction for a study of the case with four branch circles and also possibly give some insight into the behavior of the case with three branch circles.

Again most experiments behaved the same regardless of the type of circle packing used so a basic circle packing was used in the results shown. Since branch circles must be in the interior the circle packing shown in Figure 4-5 was used. The idea behind using these branched motifs to approximate discrete maps was to obtain a degree of flexibility. The motif must also be coherent if it is going to be of any use. A coherent motif with three branch circles has no flexibility. Now look at Figure 4-6.

Figure 4-6 displays the same experiment done in the previous two sections except that one variable is not shown. Following Figure 4-5, branching was randomly placed on circles 1, 4, 5, and 6 with the percentages of the extra 2π on the circles 5 and 6 shown. Clearly, the distribution that yields a coherent solution is not unique! The same experiment was repeated in Figure 4-7, Figure 4-8, and Figure 4-9 with the branching at circle 1 set to $.2(2\pi)$, $.5(2\pi)$, and $.9(2\pi)$ respectively. It appears that the four branch circle case has infinitely many solutions and that knowing one of these solutions might reveal all the solutions on at least one parameter.

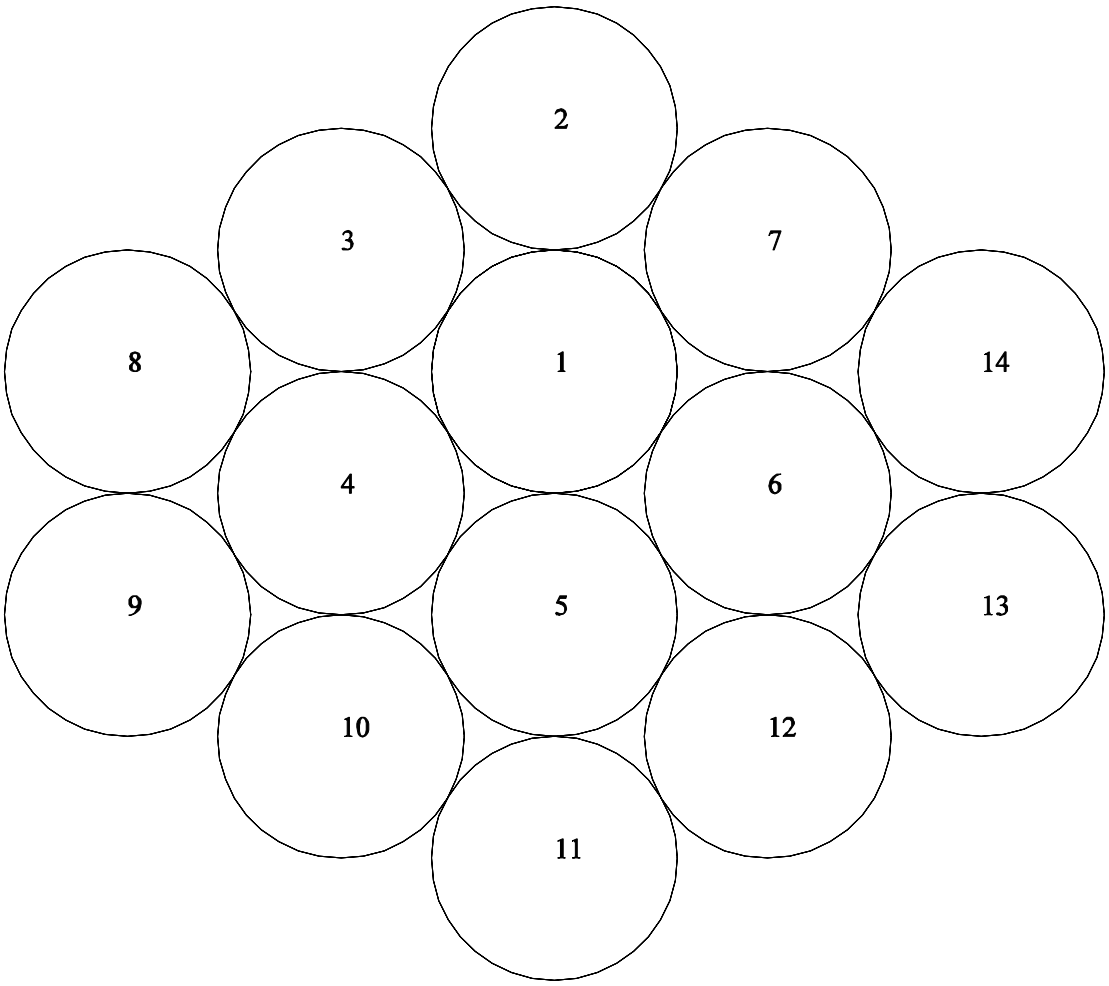

Figure 4-5: The circle packing used in the experiments with four branch circles.

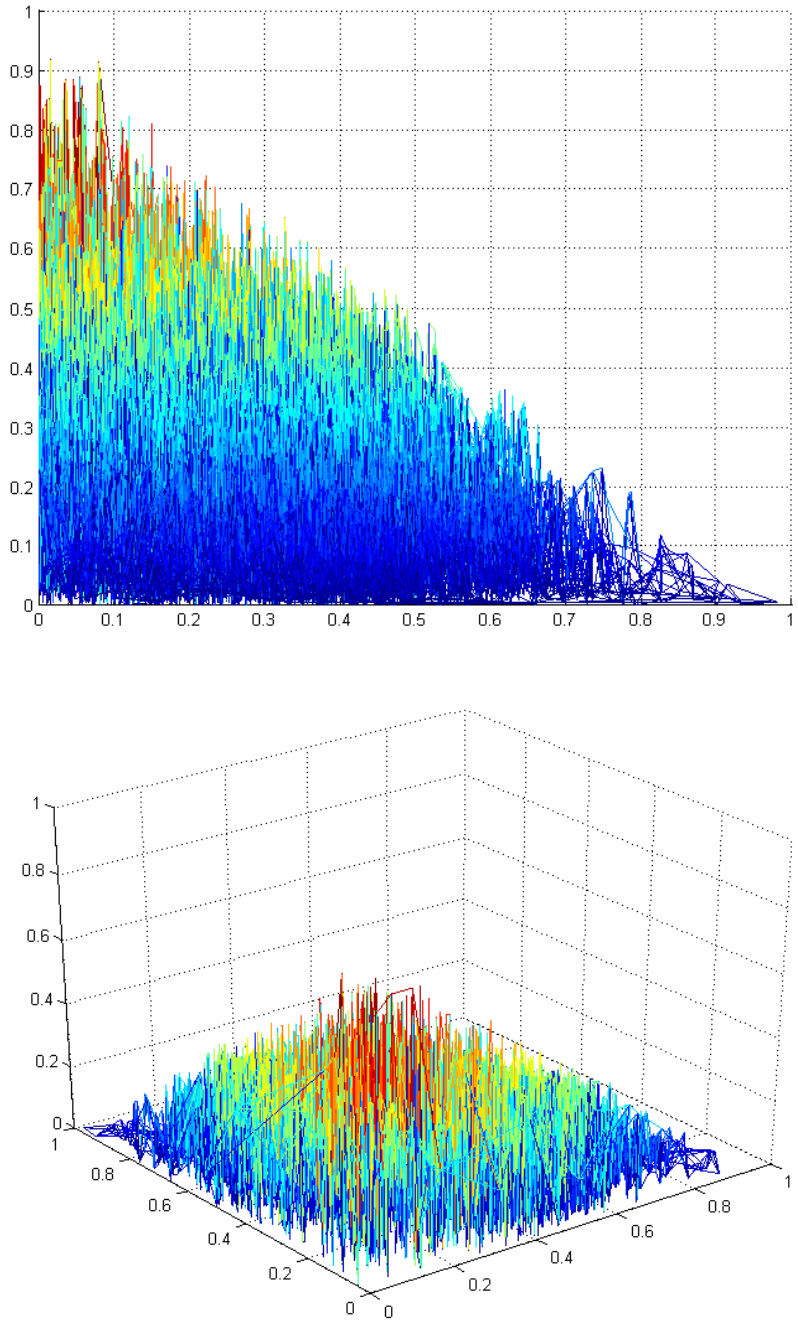

Figure 4-6: A side and angled view of 100,000 experiments on the circle packing in Figure 4-5 with four branch circles.

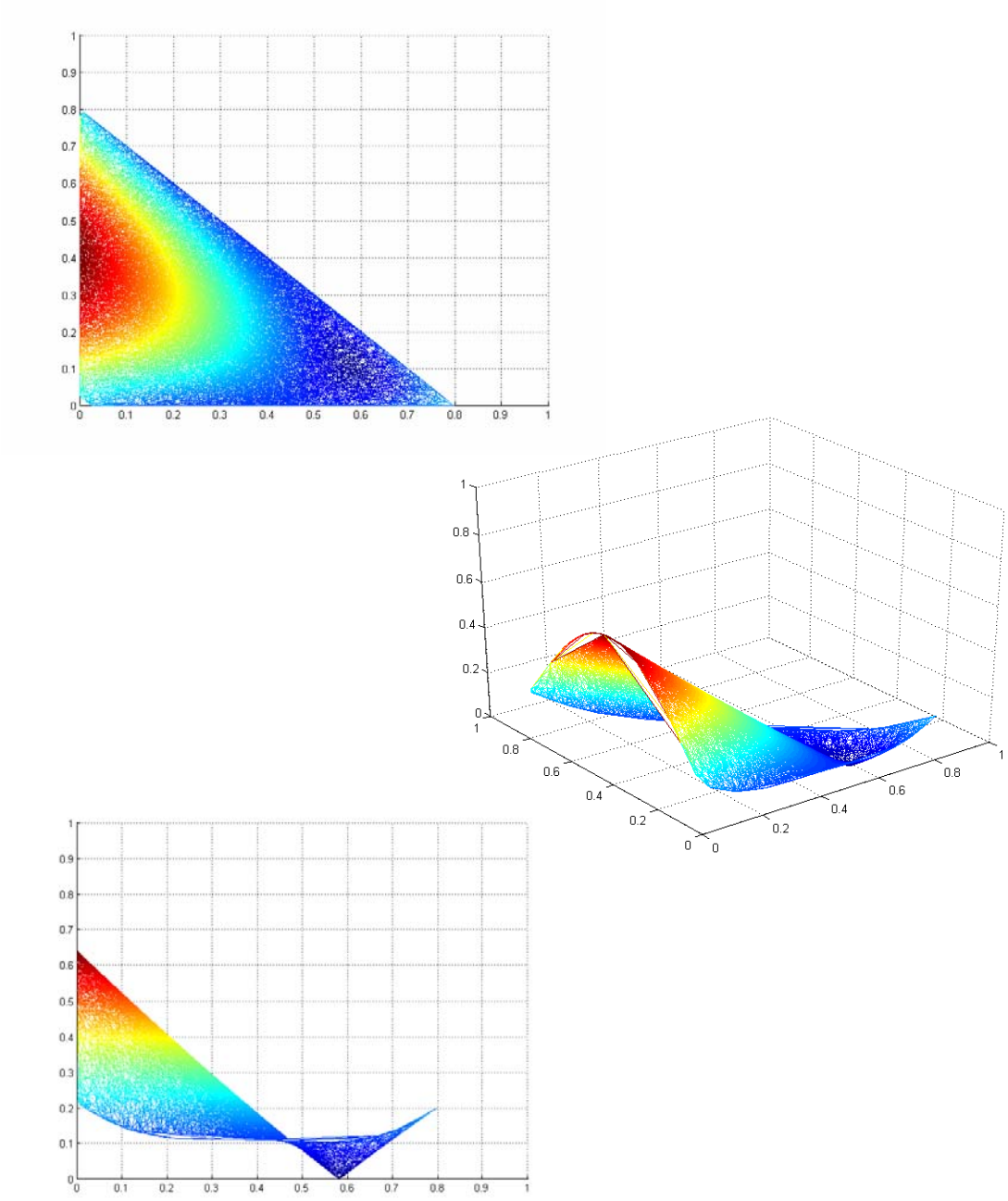

Figure 4-7: The branching at circle 1 has been set to $.2(2\pi)$. A top, angled, and side view of 100,000 experiments on the circle packing in Figure 4-5 with four branch circles is shown.

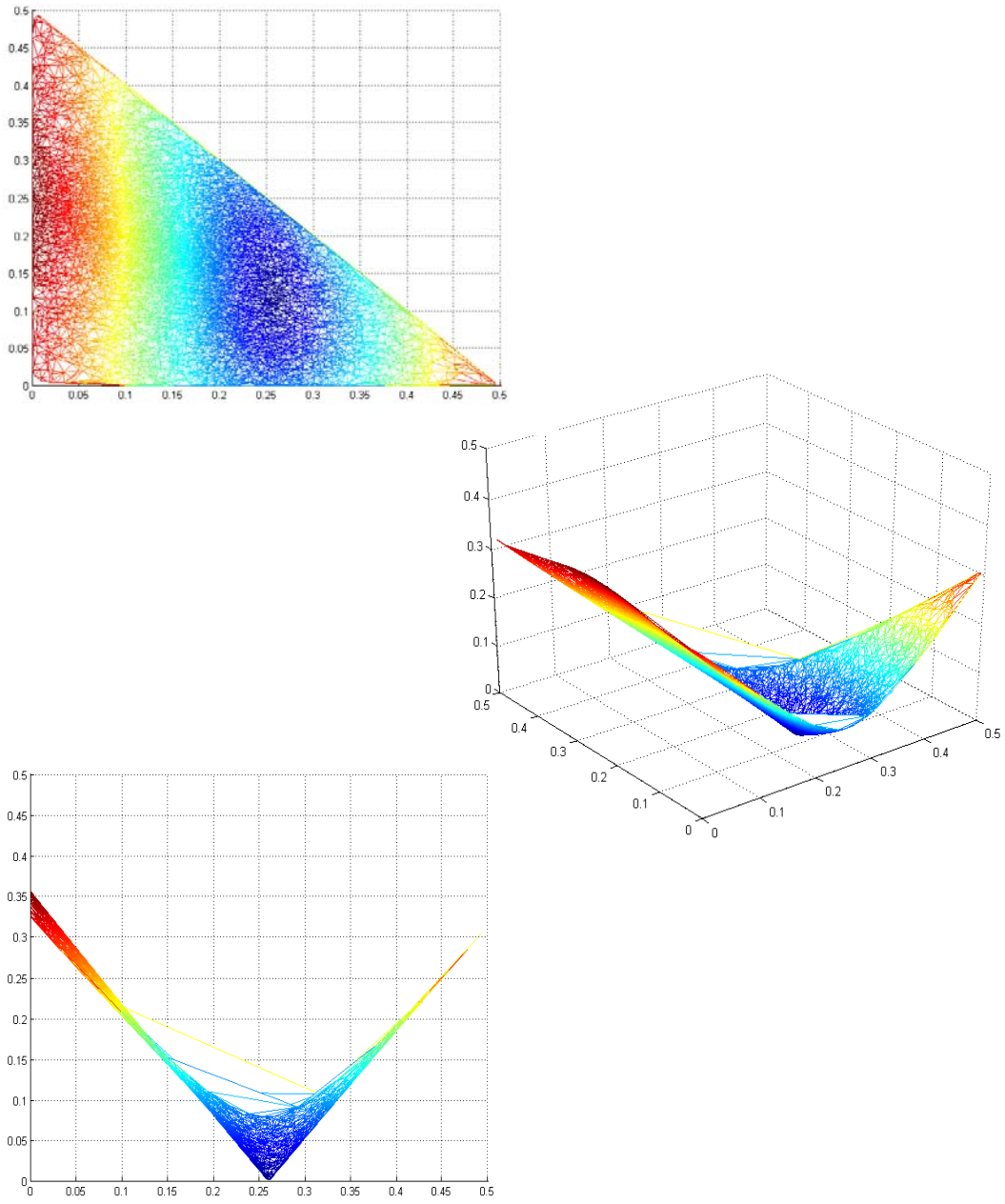

Figure 4-8: The branching at circle 1 has been set to $.5(2\pi)$. A top, angled, and side view of 30,000 experiments on the circle packing in Figure 4-5 with four branch circles is shown.

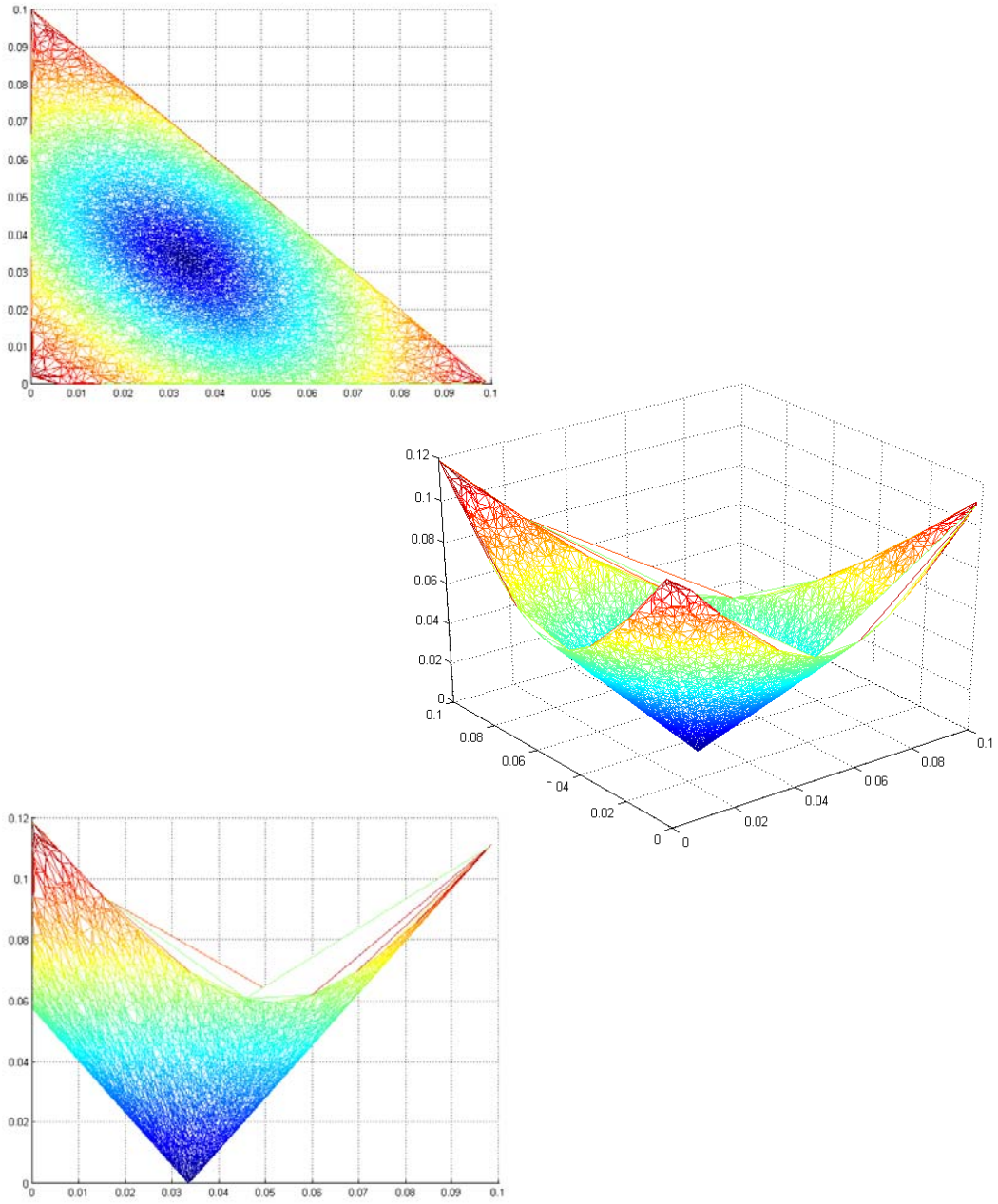

Figure 4-9: The branching at circle 1 has been set to $.9(2\pi)$. A top, angled, and side view of 30,000 experiments on the circle packing in Figure 4-5 with four branch circles is shown.

Chapter 5
Fractured Branched Motifs with Three Branch Circles

Most of the results in this section follow from relatively simple Euclidean geometry. This might seem odd since Circle Packing is usually in the service of analysis. This is, however, appropriate considering its origins since the underlying relation in a packing between its tangencies and radii is purely geometric. Many trivial geometric results involving triangles have quite complicated analytical solutions that lose not only the beauty but the essence of the problem. The computation of angle sum by cosines is not difficult but it is complicated, and solving for a particular value can be both complicated and difficult. Compound this several times with multiple tangencies and changing radii and the problem can become daunting.

Branched maps are derived from packings by simply increasing angle sums; usually all we need to do is focus on the direction of these changes and ignore the rest. So the equations involving differentials one might expect to find here are completely absent, and though this might be a little surprising it is fortunate for the writer. The methods will not only be more approachable and revealing but also more graceful. With the hope of later generalizing our results, we will investigate the branching of a special type of packing called the simple packing.

Definition 16: A *simple packing* is a circle packing with exactly three interior circles

Figure 3-2 and Figure 4-1 are both examples of simple packings. Before we begin an investigation on fractured branched maps with three branch circles we first need to show that the case with two branch circles is impossible.

Theorem 7: No fractured map with exactly two branch circles is coherent.
Proof. Recall that if a motif is coherent then every face not composed entirely of branch centers will be placed in the same location by a holonomy as it will for the trivial closed

chain. So if we follow the "rotations" occurring as a result of branching, the branch vertices must also be placed in the same location since they are part of one of these faces. Figure 5-1 illustrates how this rotation occurs. Assume that a packing has been fractured at two branch circles. Suppose the first branch circle, B_1, has branching, $b_1 = a$ where $0 < a < 2\pi$, and the second branch circle, B_2, has branching, $b_2 = c$ where $a + c = 2\pi$. Place B_1 and B_2 on the x-axis with B_1 at the origin. The total angle sum at B_1 is not an integer multiple of 2π so if we lay out the faces B_2 will be repositioned somewhere not on the axis. Now the branching at B_2 can reposition B_1 but cannot possibly reposition itself as in Figure 5-2.

The "rotations" happen because the angle sum of the branch circle is the shared vertex of all the faces in its flower, and the angle sum is greater than 2π but less than 4π. Using a similar approach we now show the following important theorem about fractured branched motifs with three branch circles.

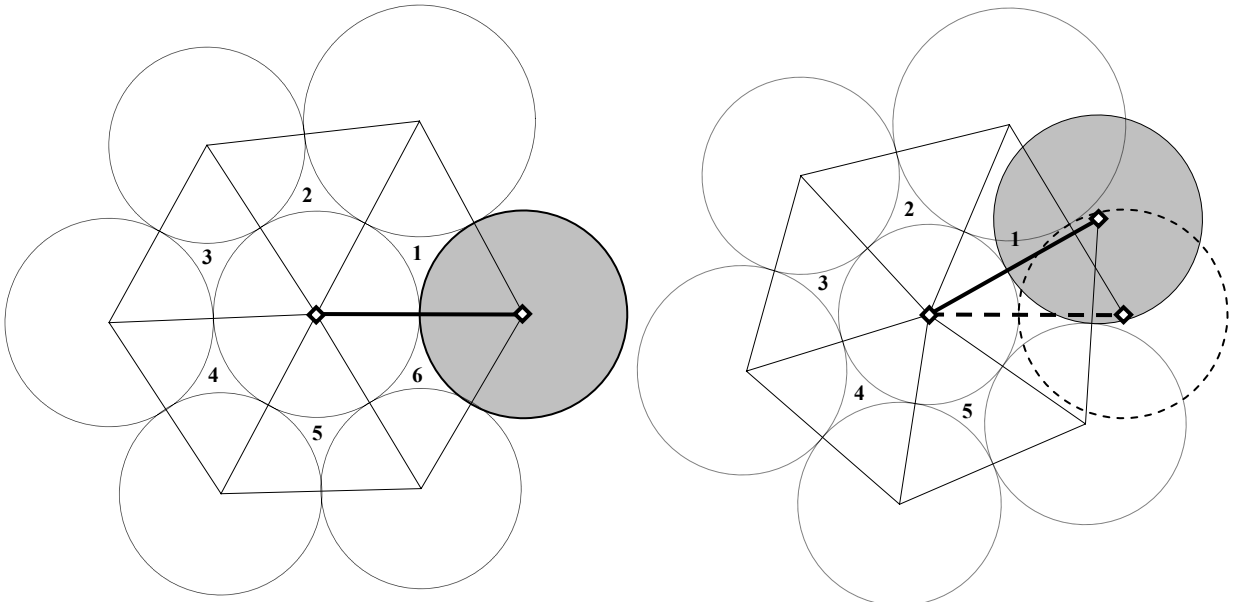

Figure 5-1: Branching the flower at its center causes the rotation of the shaded circle.

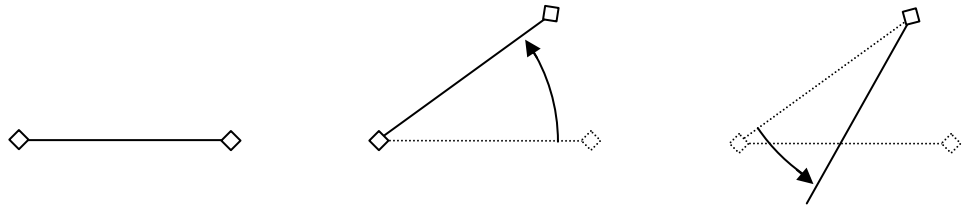

Figure 5-2: Branching a motif at two circles.

Definition 17: A *branch triangle* is the triangle formed by three branch circles.

When a motif is incoherent there will be different ways to lay out the circles. To avoid any ambiguity the branch triangle will always refer to the triangle that is found by laying down the branch circles first.

Definition 18: If *C* is a branch circle then its *branch angle* is the angle of a branch triangle with *C* at the vertex. The branch angle at branch circle C_i will be denoted α_i.

Definition 19: A *tri-branched* motif is a fractured branched motif with exactly three branch circles.

From this point forward it will be assumed that all tri-branched motifs are nontrivial. That is, each of the branch circles have a branching greater than 0.

Theorem 8: The Tri-branching Property. A tri-branched motif is coherent if and only if the branching at each circle is equal to twice its branch angle. That is, $b_i = 2\alpha_i$ for each *i*=1, 2, or 3.

Proof. Suppose a triangle, *T*, was rotated around each of its vertices by positive angles that summed to π such that the final rotation returned the triangle to its original position. So we have three rotations and three vertices. See Figure 5-3 for an example. Each

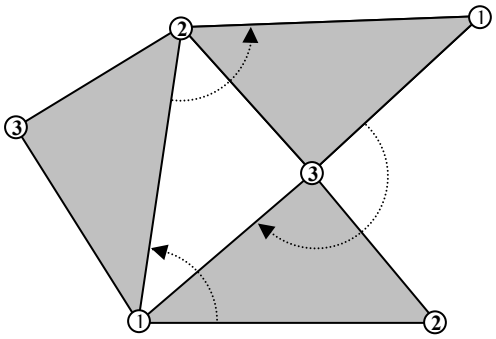

Figure 5-3: Rotations of the triangle.

rotation places *T* in a new position. Since the locations of the last triangle and the original triangle are identical we have three copies of *T*. These three triangles each share a vertex with the two other triangles and so they form a new triangle, *T',* with edges from the original triangle. A rotation occurred at each vertex so the three edges of *T'* each has an edge from *T*. Two triangles with the same sides are identical, so *T* and *T'* are identical. It follows that the rotation at a vertex is just the angle at that vertex twice, once for the triangle and once again for the identical triangle. Recall from the proof of Theorem 7 that non-integer multiples of branching cause a rotation as illustrated in Figure 5-1; so this applies directly to branched maps with exactly three branch circles. The converse follows directly.

Existence of a Coherent Tri-Branched Motif

Theorem 9: A coherent branching distribution for a tri-branched pacing exists.

Proof: The total branching on all three circles is always 2π as is twice the total of all branch angles. In both the former and latter, one value can be determined from the values of the other two. Below are two simplexes. The simplex in Figure 5-4 represents the branch distribution where the x-axis is the distribution of branching at one branch circle and the y-axis is the distribution at one of the other branch circles. The x-axis and y-axis in the adjacent simplex represent the doubled branch angle for the same circles. Branching a packing and then applying the packing algorithm will yield an associated branch triangle. That is, the circle packing algorithm computes radii for the associated

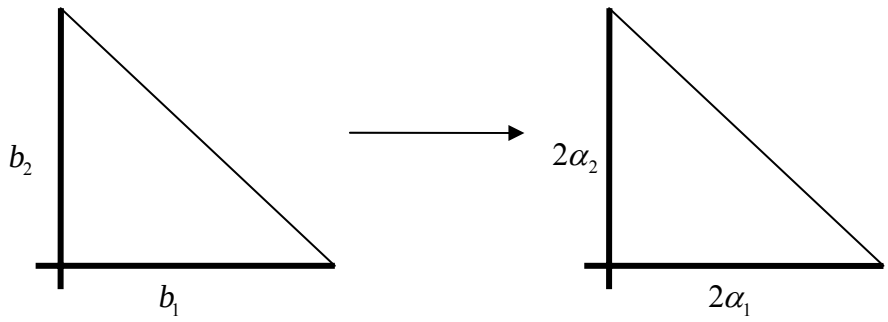

Figure 5-4: Map from the simplex of branch distribution onto the simplex of branch angles.

complex and hence the branch angles. The angles are a continuous function of the prescribed branching, so we can describe a continuous function from one simplex onto the other. Identifying the two simplexes, the function is a map from a compact surface into itself. So then by Brouwer's fixed point theorem there will be at least one fixed point. Hence by the angle condition at least one distribution will produce a coherent packing. Note that Theorem 9 applies to any circle packing, not just simple packings.

Uniqueness

As the experimental data in Chapter 4 suggests, the coherent distribution in a simple packing is unique. When a circle packing is branched its complex is unchanged. The only way left to change the angle sums is by manipulating the radii. In a simple packing there are only three interior circles so all the non-branched neighbors of the branch circle are border circles whose radii will remain fixed. The simple packing is thus branched by changing only the radii of the branch circles. As an immediate result of the law of cosines, any change in branch distribution results in at least one branch radius changing, and any change in a branch circle's radius will affect the branching of both its neighboring branch circles.

Definition 20: A non-branched circle that is tangent to more than one branch circle is a *connecting circle*.

When there are three branch circles, a connecting circle is tangent to two branch circles, and any two connecting circles are tangent to a single branch circle. In general, ownership will be used to imply univalent tangency. For example, saying that "connecting circle A is branching circle's B's connecting circle" or "connecting circle A belongs to branching circle B" means that the complex assigns A and B to be tangent. Connecting circles will be identified with the notation, $\overset{i}{C}_v^{\,j}$, where *i* and *j* are the connecting circle's branch circles and *v* is the vertex of the connecting circle. An example is shown in Figure 5-5. Ownership is determined by the complex and is unchanged by branching.

Definition 21: The *partial angle sum* of a branch circle is the sum of angles in the branch circle's flower that is formed by non-branch circles. This is a local non-closed chain from one of the branch circle's connecting circles to its other connecting circle. See Figure 5-6 for an example.

Definition 22: The *connection angle* is the difference between the partial angle sum and 2π. That is, $2\pi -$ partial angle sum $=$ *connection angle*. With coherent and incoherent packings it may be possible for the partial angle sum to exceed 2π so the connection angle will sometimes be negative where the sign just represents the angles' orientation as usual. The connection angle will be represented with the notation $\overset{i}{\underset{v}{\forall}}\overset{j}{}$ where *i* and *j* are the connection circles and *v* is the branch circle. It will usually be more convenient to refer to the connection angle of a branch circle instead of its partial angle sum.

Definition 23: A *branch-connection angle* is formed by one of a branch circle's branched neighbors and their shared connection circle with the branch circle as the vertex. These are the angles for branch circle B_1 with branched neighbors B_2 and B_3. Each branch circle has two connection circles and two branched neighbors so every branch circle will have exactly two branch-connection angles.

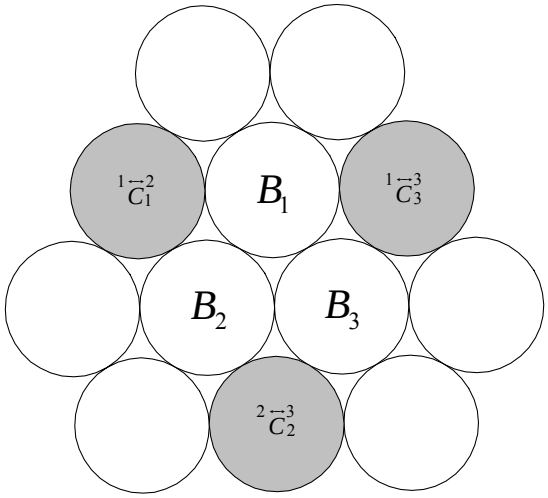

Figure 5-5: The connection circles are shaded.

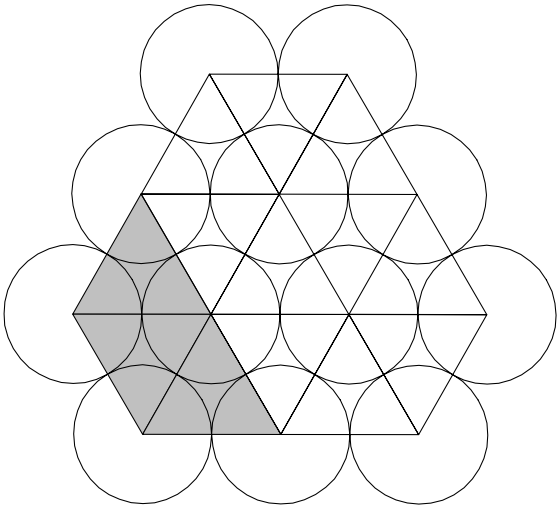

Figure 5-6: The partial angle sum of an interior circle is shaded.

In a non-fractured branched motif, the radius of a branch circle uniquely determines the angle between its connection circles. In a fractured branched motif the radius of a branch circle does not uniquely determine its angle sum since neighboring branch circles may have their radii increased or decreased. A branch circle's connection angle is completely independent of the other branch circle radii since they are not included in the partial angle sum.

The partial angle sum is like a belt wrapped around the branch circle. The length of the belt is unchanged so the size of the waist determines where the ends of the belt will be. The connection angle will change positively if the branch circle increases and negatively if the branch circle decreases. An example of the latter is shown in Figure 5-7.

Theorem 10: In a simple tri-branched packing, there is only one distribution that yields a coherent packing.

Proof: Suppose that the coherent branched packing of a simple packing is not unique. We can assume a coherent packing exists and view a second coherent packing as having been changed from the first through manipulation of branch radii. When the radii ratio of two tangent circles changes the position of any third mutually tangent circle also changes. The

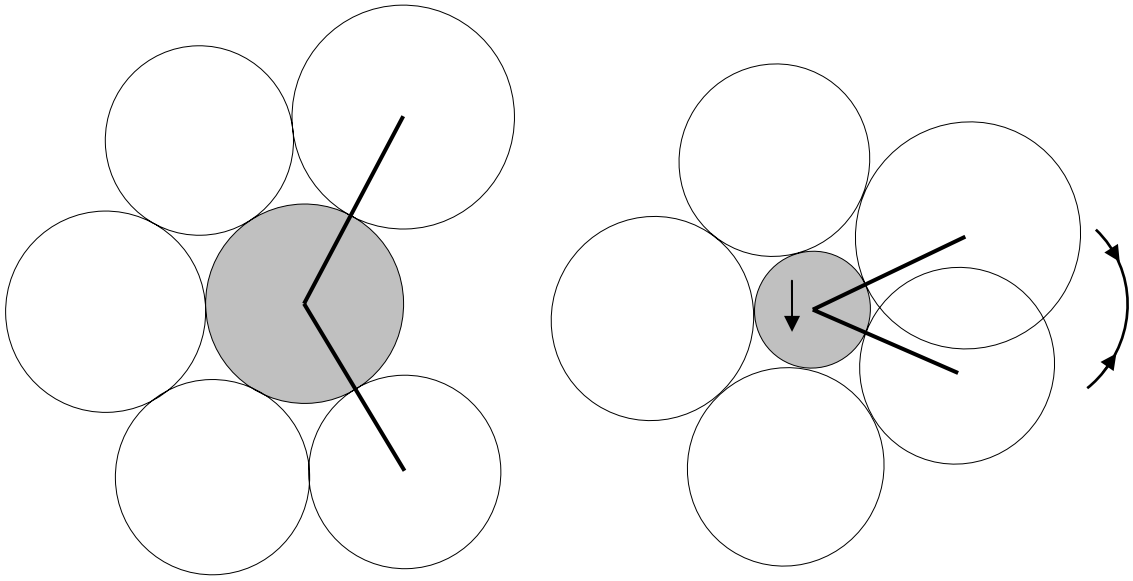

Figure 5-7: The connection angle changes negatively when the branch circle decreases.

vertex of a third tangent circle will lie on a hyberbola that has foci at the vertices of the two base circles, and a curvature defined by the difference in radii between the two base circles. This curve is a straight line if the difference between the two base circles is zero, and becomes more curved if the difference grows, bending away from the larger circle as in Figure 5-8.

Lemma 1: If two circles are tangent in a circle packing then they will be tangent in a coherent packing if they are branched.

Proof. Two circles must be tangent to find the location of a third tangent circle, and in a coherent packing two tangent branch circles will share at least one face with a non-branched circle. So if they are not tangent then the motif cannot be coherent.

If we change a branch circle's radius we set two forces in opposition. The connection angle will be determined completely by the radii, but changing the radius also changes the tangency relations.

Lemma 2: If the total amount of branching is 2π then changing the branching in a simple motif will always result in at least one branch circle radius changing positively and another changing negatively.

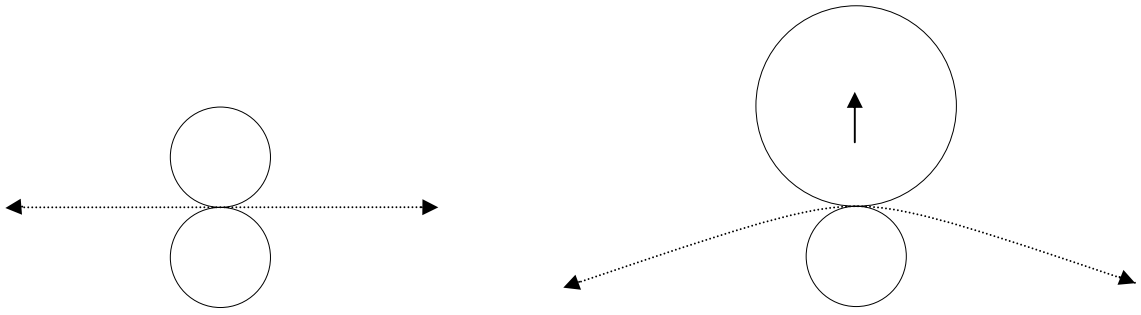

Figure 5-8: A bend in the tangency-hyperbola as a result of a change in the ratio of the radii of the tangent circles.

Proof. If all the branch circle radii are increased than all their partial angle sums will decrease. There are then three faces in each flower that are left unaccounted for, the branch triangle and the two faces that each share an edge with the branch triangle (the branch-connection angle). These faces are each composed of two branch circles and one connection circle. Let the branch circles be B_i. The connection circles' radii will not change so the angle $\overset{B_i}{\underset{i\,\overline{C_v}\,j}{\bigvee}}\overset{B_j}{}$ will increase since both B_i and B_j increase. The sum of the remaining angles in each of these triangles will then decrease. The branch angle will not affect the sum of the branch circle's angle sum since each branch circle has a vertex in the triangle. So the total angle sum decreases, which is a contradiction. It can be similarly shown that all the branch radii cannot decrease and that only one branch radius cannot change.

Now we proceed in the proof of Theorem 10. By Lemma 2, changing the branching in a coherent tri-branched packing will result in one branch radii that has been increased and another that has been decreased. The remaining branch circle will be increased, decreased, or unchanged.

Consider the case when one branch circle is unchanged. Let the decreasing branch circle be called B_1, the increasing branch circle B_2, and the unchanged circle B_3. The ratios of the radii of B_1 to B_2 and the radii of B_1 to B_3 both changes such that the tangency-hyperbolas created by B_1 with B_2 and B_1 with B_3 will both bend towards B_1 since by Lemma 1 all these circles will be tangent. This will increase the connection angle.

This is a contradiction since decreasing the radius of a branch circle will increase its partial angel sum and thus decrease its connection angle. Figure 5-9 and Figure 5-10 illustrate this when the partial angle sum is less than 2π, and Figure 5-11 and Figure 5-12 illustrate this when the partial angle sum is greater than 2π. The remaining two cases work out similarly.

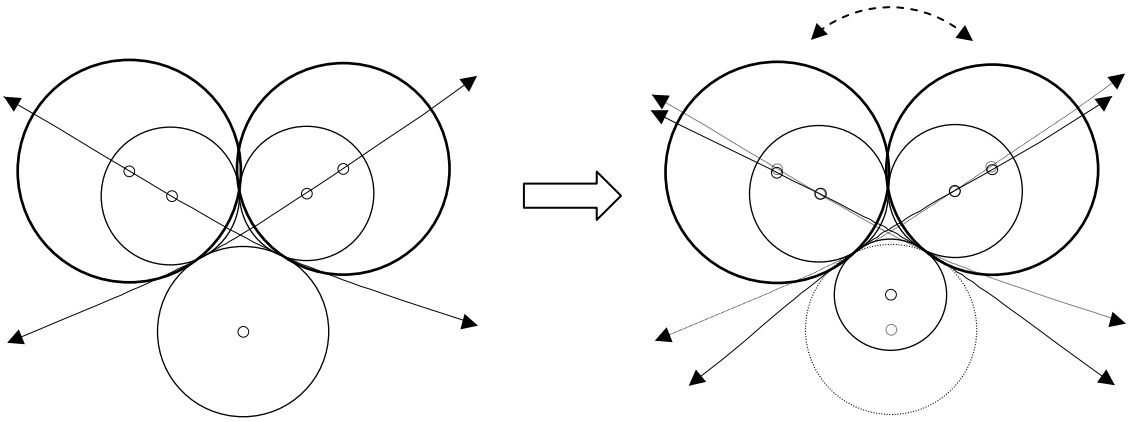

Figure 5-9: The tangency-hyperbolas change as a result of the change in ratio of the radii when the partial angle sum is less than 2π .

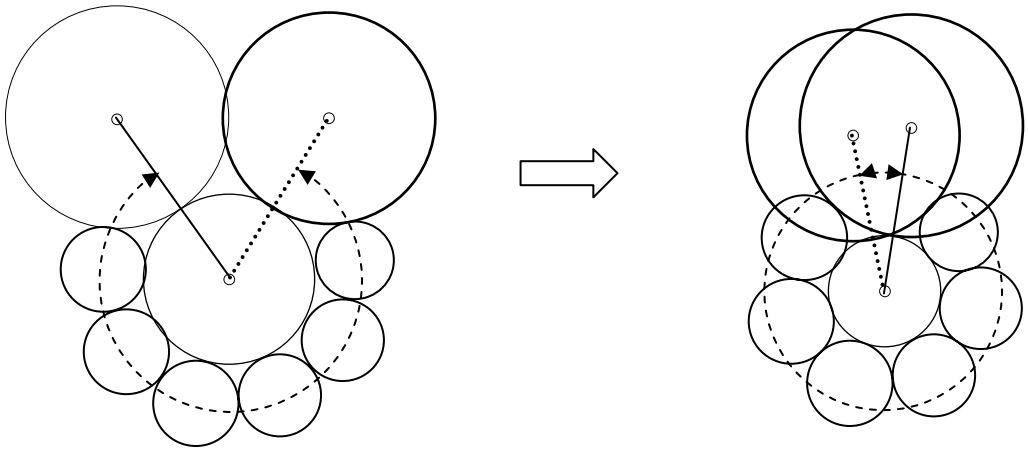

Figure 5-10: Change in the connection angle when the partial angle sum is less than 2π .

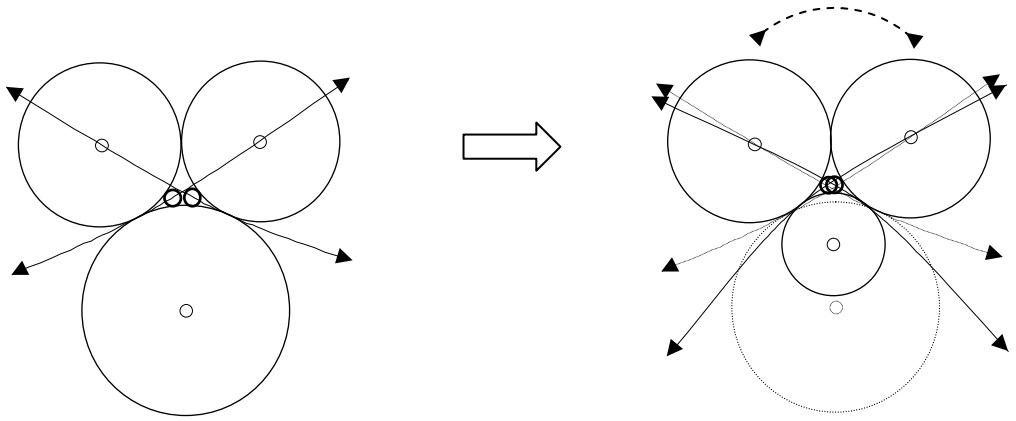

Figure 5-11: The tangency-hyperbolas change as a result of the change in ratio of the radii when the partial angle sum is greater than 2π .

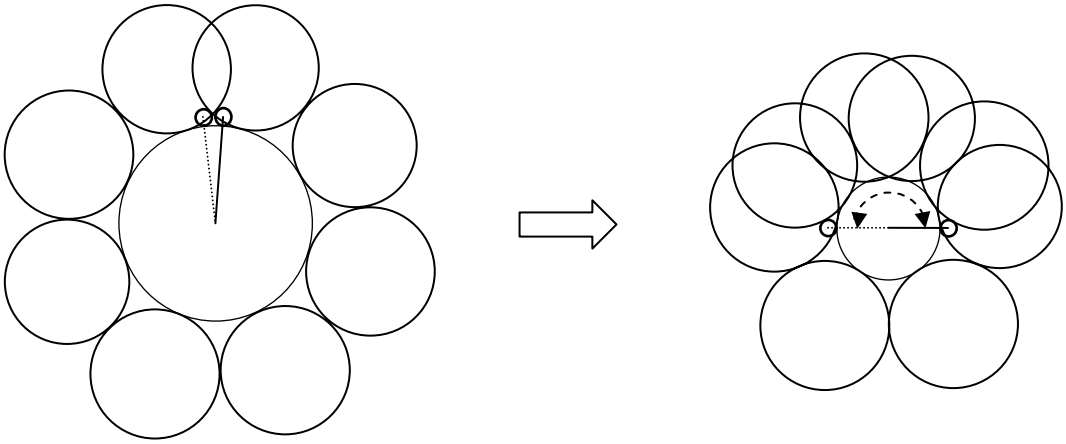

Figure 5-12: The change in the connection angle is positive when the partial angle sum is greater than 2π .

It is possible to make these hyperbolas with a Euclidean construction. Essentially the same argument can be made using the faces. Refer to Figure 5-13 for an illustration of the angles described here. The branching at a branch circle is just the sum,

$$b_1 = \underset{B_1}{\overset{B_2}{\vee}}\overset{B_3}{} + \underset{B_1}{\overset{B_2}{\vee}}\overset{{}^1\vec{C}^2}{} + \underset{B_1}{\overset{B_3}{\vee}}\overset{{}^1\vec{C}^3}{} + (\textit{partial angle sum}) - 2\pi$$

$$\Rightarrow b_1 = \underset{B_1}{\overset{B_2}{\vee}}\overset{B_3}{} + \underset{B_1}{\overset{B_2}{\vee}}\overset{{}^1\vec{C}^2}{} + \underset{B_1}{\overset{B_3}{\vee}}\overset{{}^1\vec{C}^3}{} - \overset{{}^1\vec{C}^2}{\underset{B_1}{\forall}}\overset{{}^1\vec{C}^3}{}$$

If the motif is coherent then by the tri-branching property we have the equality

$$2\cdot \underset{B_1}{\overset{B_2}{\vee}}\overset{B_3}{} = \underset{B_1}{\overset{B_2}{\vee}}\overset{B_3}{} + \underset{B_1}{\overset{B_2}{\vee}}\overset{{}^1\vec{C}^2}{} + \underset{B_1}{\overset{B_3}{\vee}}\overset{{}^1\vec{C}^3}{} - \overset{{}^1\vec{C}^2}{\underset{B_1}{\forall}}\overset{{}^1\vec{C}^3}{}$$

Which gives the following equation for the connection angle in a coherent motif,

$$\overset{{}^1\vec{C}^2}{\underset{B_1}{\forall}}\overset{{}^1\vec{C}^3}{} = -\underset{B_1}{\overset{B_2}{\vee}}\overset{B_3}{} + \underset{B_1}{\overset{B_2}{\vee}}\overset{{}^1\vec{C}^2}{} + \underset{B_1}{\overset{B_3}{\vee}}\overset{{}^1\vec{C}^3}{}.$$

As before, assume that one branch circle decreases and that the remaining two do not decrease. If B_1 decreases then $\underset{B_1}{\overset{B_2}{\vee}}\overset{B_3}{}$, $\underset{B_1}{\overset{B_2}{\vee}}\overset{{}^1\vec{C}^2}{}$, and $\underset{B_1}{\overset{B_3}{\vee}}\overset{{}^1\vec{C}^3}{}$ each increase since the connection circle does not change and the other two branch circles either increase or do not change. Because B_1 decreases the connection angle must decrease. For this to happen the change in B_1's branch angle, $\underset{B_1}{\overset{B_2}{\vee}}\overset{B_3}{}$, must exceed the combined change in $\underset{B_1}{\overset{B_2}{\vee}}\overset{{}^1\vec{C}^2}{}$ and $\underset{B_1}{\overset{B_3}{\vee}}\overset{{}^1\vec{C}^3}{}$.

This cannot occur without relaxing the univalent tangency requirement since any change in $\underset{B_1}{\overset{B_2}{\vee}}\overset{B_3}{}$ will cause the exact same change in $\underset{B_1}{\overset{B_2}{\vee}}\overset{{}^1\vec{C}^2}{}$ and $\underset{B_1}{\overset{B_3}{\vee}}\overset{{}^1\vec{C}^3}{}$. From Figure 5-13, $\underset{B_1}{\overset{B_2}{\vee}}\overset{B_3}{} = a + b$. A decrease of B_1 and a non-negative change of B_2 and B_3 will guarantee that both angles *a* and *b* will increase. Similarly both $\underset{B_1}{\overset{B_2}{\vee}}\overset{{}^1\vec{C}^2}{} - b$ and $\underset{B_1}{\overset{B_3}{\vee}}\overset{{}^1\vec{C}^3}{} - c$ will also increase because neither connection circle changes. So again a change in a

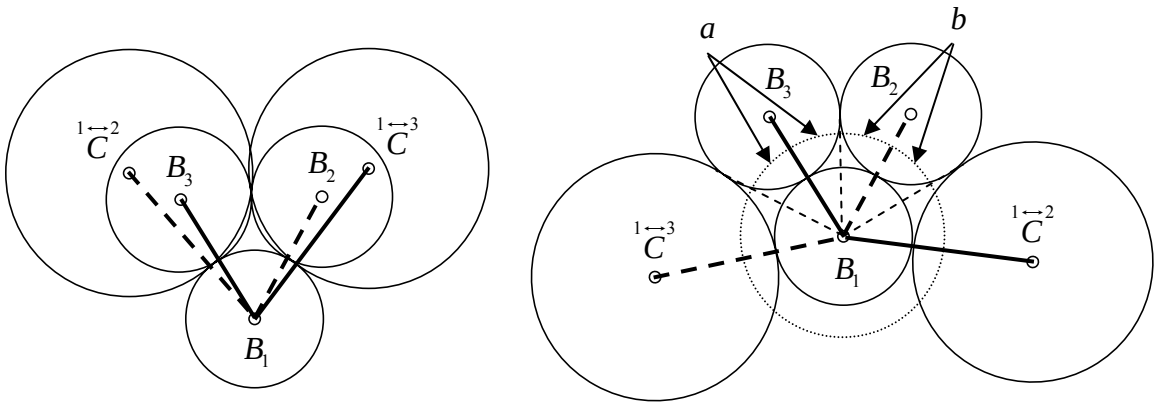

Figure 5-13: The relationship between the branch angles and connection angles is very rigid in a coherent packing.

branch circle's radii requires that the connection circles move in one direction according to tangencies and the opposite direction according to its partial angle sum.

From Lemma 1one might infer that making the distinction between a coherent packing and a circle packing is unnecessary. The difference is rather subtle. In a coherent packing, branching has to occur such that each circle retains its tangency and each branch circle has the correct extra angle sum. A circle packing has the added property that orientation is preserved.

Imagine that the branching happens in a continuous process beginning with a packing and slowly transforming into a coherent branched packing. As a circle is branched its tangent branch circles begin to pass through each other. Their radii are also in the process of changing since they are also being branched, but there are only two possible places for them to be tangent. The first one is their initial point of tangency which is gone as soon as branching begins. The second is the point of tangency just after they completely pass through each other. At this second point the motif is not a packing because orientation has not been preserved at the branch circles.

If we place the circles at this point, the orientation of the two branch circles has been "flipped." This is precisely where Theorem 8, the tri-branching property, enters. The "flip" allows the extra angle sum to be added while preserving tangency, and is the reason the extra angle sum must be exactly *twice* the branch angle.

Chapter 6
An Algorithm

A tri-branching coherent motif exists and is unique. Now how do we find this solution? The tri-branching property tells us exactly what the branching needs to be in relation to the branch radii, however these radii change whenever the angle sums are changed! The branch angle is very fluid, morphing with every little change of the branching. Since the partial angle sums of a branch circle in the triangle change independently of the changes in the other branch circles, a small change in the branch triangle could result in a large change in angle sums. If an incoherent packing is repacked according to its branch angles the branch angles change because the branching changes the radii, however the resulting motif will be "less" incoherent then its predecessor.

First we need a different method of measuring incoherency from the one used in Chapter 4. The problem with that method is that the motif initially becomes "worse" as the distribution moves away from the trivial solutions, and determining where it begins to improve creates a problem. Since the motif is coherent when the tri-branching property is met, we can instead use the sum of the differences of branch angles and branching as a way of measuring error. Call the error E where $E = |b_1 - 2\alpha_1| + |b_2 - 2\alpha_2| + |b_3 - 2\alpha_3|$. By evaluating branch angles and repacking according to the branch angle we are able to chase down the solution as close as we like. The process is pleasingly simple.

The Tri-branching Algorithm

1. Branch a packing at three circles such that $b_i + b_j + b_k = 2\pi$.
2. If $E = 0$ then the packing is coherent. If $E \neq 0$ then set $b_i = 2\alpha_i, b_j = 2\alpha_{j,}$ and $b_k = 2\alpha_k$ and repack.
3. Repeat step 2 until $E = 0$.

Theorem 11: In The Tri-branching Algorithm the error, *E*, converges to 0.

Before proving the algorithm, let us first look at some experiments. Using E as the z-axis with an experiment similar to those described in Chapter 4, and using the same circle packing as the one used in Figure 4-1 gives the graphs in Figure 6-1.

Here, any distribution moving the simplex away from a trivial solution results in less error, and any movement from an incorrect distribution towards the solution also results in less error. It can be difficult to visualize an incoherent packing since there is by definition no consistent way to draw them. The program "Circlepacking" will draw an incoherent packing by relaxing external tangency.

This can create difficulty when trying to measure the error of a motif since this loses the relation between the complex and radii. We will describe a simple incoherent packing by first laying down the branch face and then laying down the flowers of each branch circle such that all their petals are tangent to the center of their flowers. If the motif is incoherent then the connection circles will not all be laid down on the same location, resulting in as many as six locations for three circles or, equivalently, two locations for each connection circle.

To simplify things, only the branching circles and connection circles are shown. Each branch circle's flower can be rotated (without changing any angles) such that each branch circle places at least one connection circle in the correct position, tangent to both its branch circles. Figure 6-2 shows how this can be done.

First we need to show that the second step of the algorithm moves the connection circles in the correct direction. Assume we describe a motif as defined above. By the tri-branching property,

$2 \cdot \overset{B_2}{\underset{B_1}{\vee}} \overset{B_3}{} = \overset{B_2}{\underset{B_1}{\vee}} \overset{B_3}{} + \overset{B_2}{\underset{B_1}{\vee}} \overset{{}^1\vec{C}^2}{} + \overset{B_3}{\underset{B_1}{\vee}} \overset{{}^1\vec{C}^3}{} - \overset{{}^1\vec{C}^2}{\underset{B_1}{\forall}} \overset{{}^1\vec{C}^3}{}$ if and only if the flower at B_1 is coherent.

Which gives the following equation for the connection angle in a coherent motif,

$$\overset{{}^1\vec{C}^2}{\underset{B_1}{\forall}} \overset{{}^1\vec{C}^3}{} = -\overset{B_2}{\underset{B_1}{\vee}} \overset{B_3}{} + \overset{B_2}{\underset{B_1}{\vee}} \overset{{}^1\vec{C}^2}{} + \overset{B_3}{\underset{B_1}{\vee}} \overset{{}^1\vec{C}^3}{} .$$

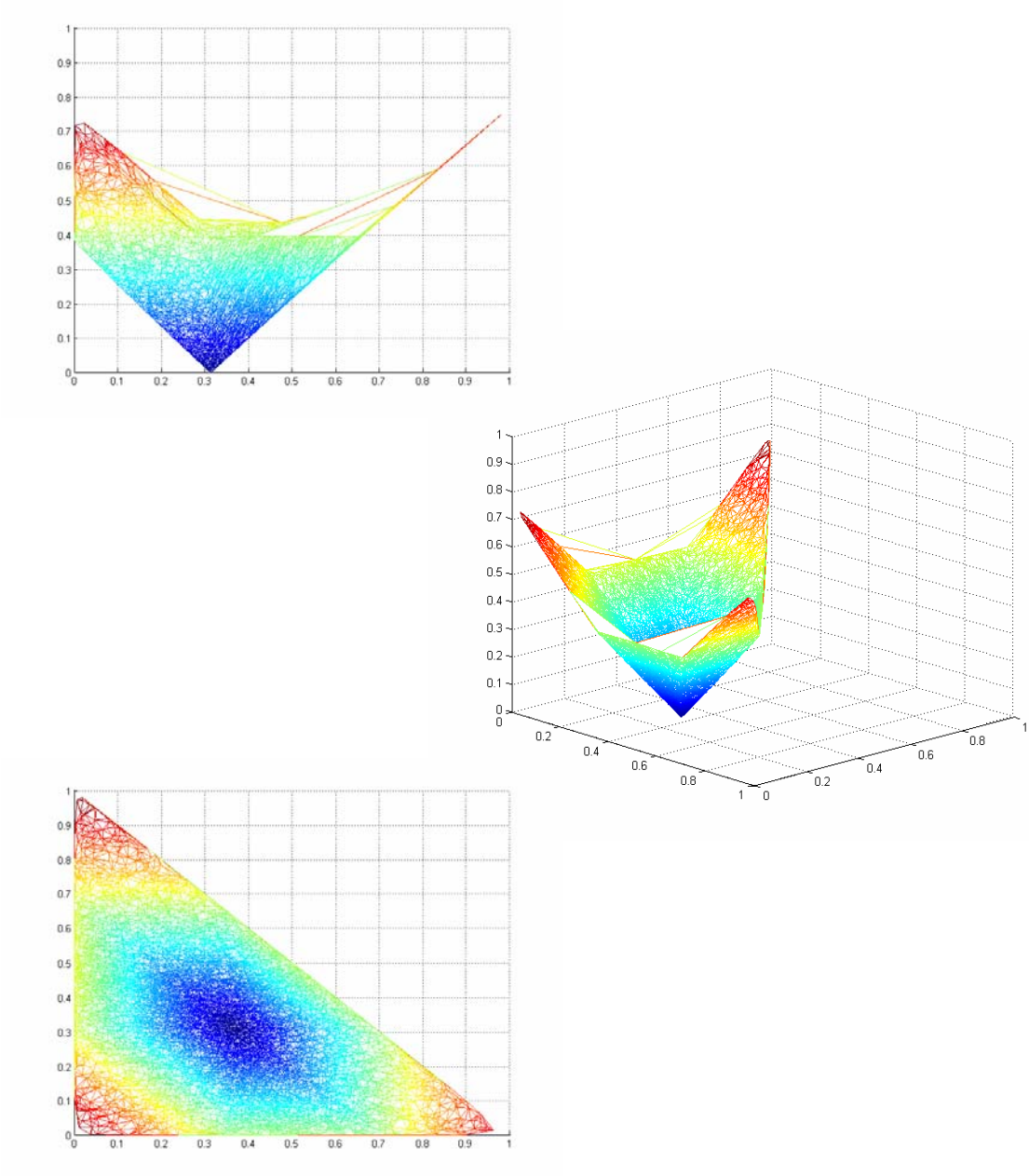

Figure 6-1: A side, top, and angled perspective of 10,000 experiments of the branching distributed between three circles using *E* to measure incoherency.

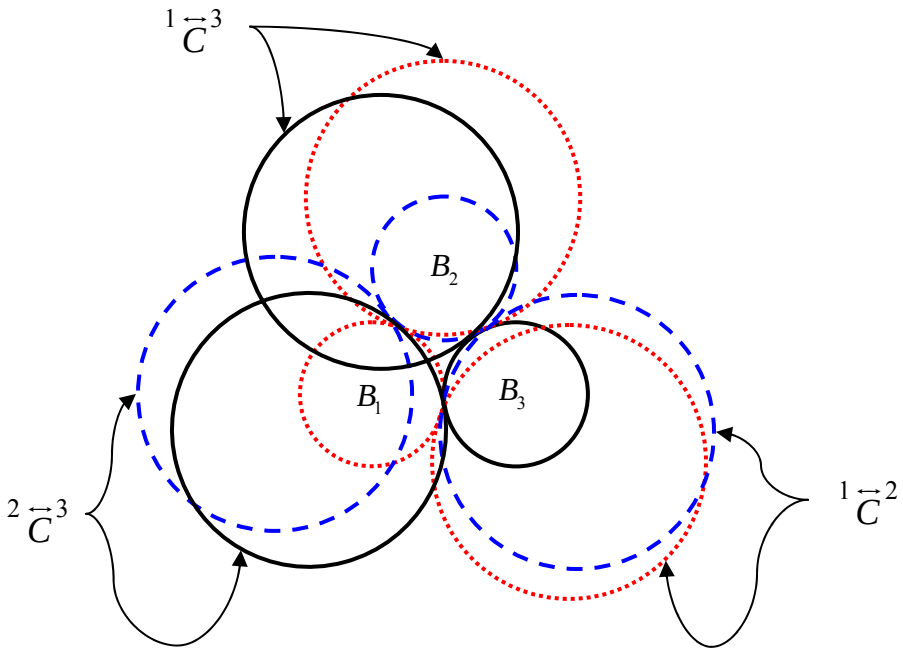

Figure 6-2: A description of an incoherent packing.

As in Chapter 5,

$$b_1 = \overset{B_2}{\underset{B_1}{\vee}}\overset{B_3}{} + \overset{B_2}{\underset{B_1}{\vee}}\overset{^{1}\overleftrightarrow{C}^{2}}{} + \overset{B_3}{\underset{B_1}{\vee}}\overset{^{1}\overleftrightarrow{C}^{3}}{} + (\textit{partial angle sum}) - 2\pi$$

$$\Rightarrow b_1 = \overset{B_2}{\underset{B_1}{\vee}}\overset{B_3}{} + \overset{B_2}{\underset{B_1}{\vee}}\overset{^{1}\overleftrightarrow{C}^{2}}{} + \overset{B_3}{\underset{B_1}{\vee}}\overset{^{1}\overleftrightarrow{C}^{3}}{} - \overset{^{1}\overleftrightarrow{C}^{2}}{\underset{B_1}{\forall}}\overset{^{1}\overleftrightarrow{C}^{3}}{}$$

Suppose that as in Figure 6-3 the connection angle is to large. Following Figure 6-3, it is clear that any such motif is incoherent and that $\overset{^{1}\overleftrightarrow{C}^{2}}{\underset{B_1}{\forall}}\overset{^{1}\overleftrightarrow{C}^{3}}{} > -\overset{B_2}{\underset{B_1}{\vee}}\overset{B_3}{} + \overset{B_2}{\underset{B_1}{\vee}}\overset{^{1}\overleftrightarrow{C}^{2}}{} + \overset{B_3}{\underset{B_1}{\vee}}\overset{^{1}\overleftrightarrow{C}^{3}}{}$. Which implies that $2\cdot\overset{B_2}{\underset{B_1}{\vee}}\overset{B_3}{} > b_1 = \overset{B_2}{\underset{B_1}{\vee}}\overset{B_3}{} + \overset{B_2}{\underset{B_1}{\vee}}\overset{^{1}\overleftrightarrow{C}^{2}}{} + \overset{B_3}{\underset{B_1}{\vee}}\overset{^{1}\overleftrightarrow{C}^{3}}{} - \overset{^{1}\overleftrightarrow{C}^{2}}{\underset{B_1}{\forall}}\overset{^{1}\overleftrightarrow{C}^{3}}{}$, meaning that by the tri-branching property the branching at this circle needs to be increased.

Similarly for any branch circle changing the branching according to the branch angle will move each of the connection circles in the right direction. The question is whether it will move it too much, creating more error than we were trying to correct, or if E will eventually converge to 0.

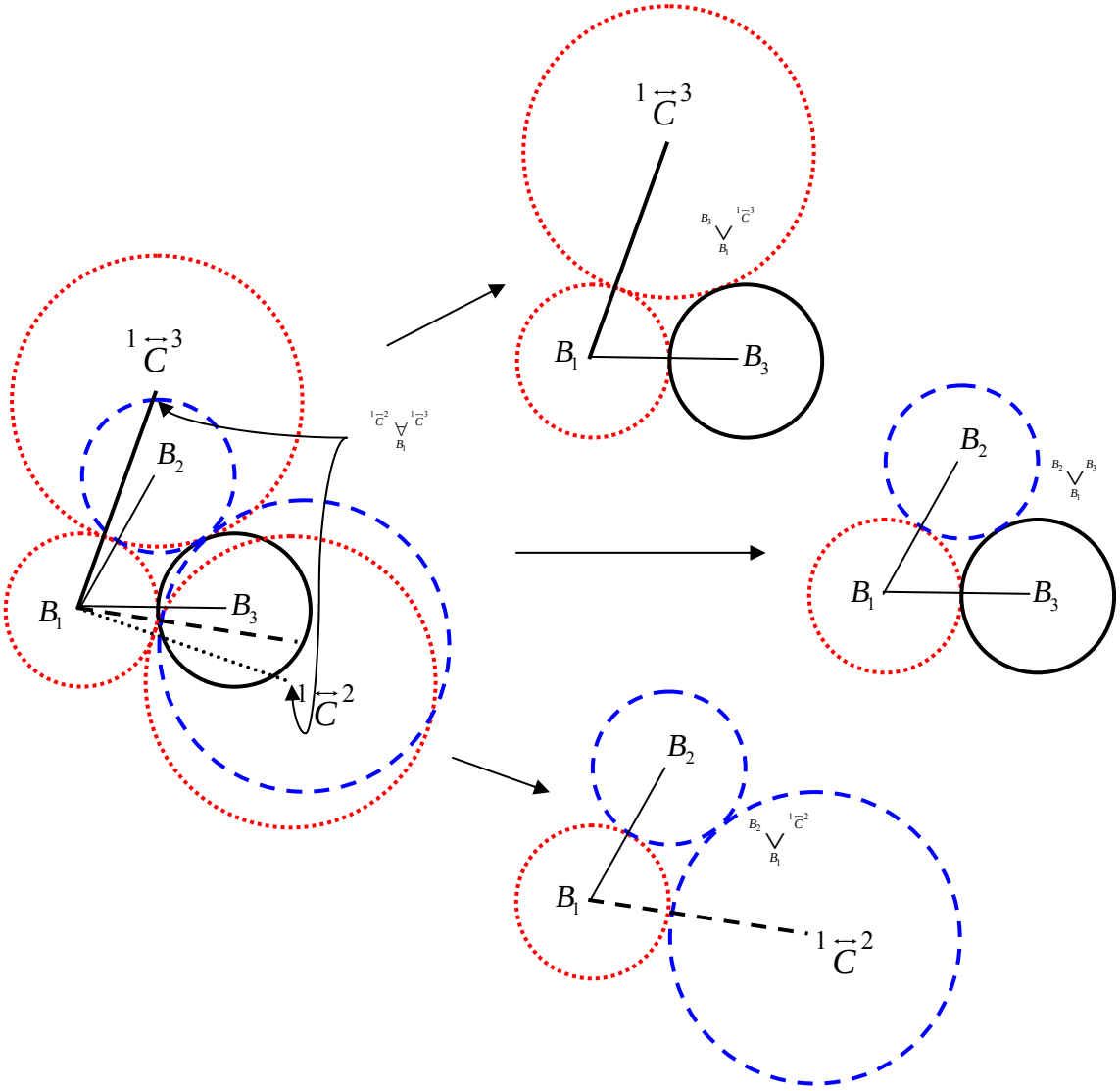

Figure 6-3: Angles in a coherent motif.

The graph in Figure 6-4 is the algorithm applied to the circle packing in Figure 4-1. Branching according to the branch angles changes the branch angles, but these angles move less and less the more times the algorithm is repeated. All experiments performed using the algorithm behaved similarly. This graph suggests that the algorithm not only converges but that in fact changing the branching by only a fraction in the correct direction will improve the error.

Now we will show that E converges to 0. The motif can be organized by laying down the branch circles first, then the connection circles, and then laying down the faces for border circles using their branch circle and one of its connection circles for orientation.

The result shown in Figure 6-5 is similar to the description illustrated by Figure 6-2, but the error has been moved to the non-connection border circles. Assume we have tri-branched a packing, branching the circles $B_1, B_2,$ and B_3, and that $E \neq 0$. The tri-branching property fails at one or more of these circles. So then $b_i - 2\alpha_i = \theta_i$ for $\theta_i \geq 0$ and $i = 1, 2,$ or 3. Setting each $b_i' = 2\alpha_i$ may give new branch angles which we will denote, α_i'. Increasing or decreasing the angle sum of one of the branch circles can be done by changing the radius of the branch circle itself or by changing the radii of its branched neighbors.

The former causes an angle change for all of the faces in the branch circle's flower while the latter causes the branch triangle and both its branch-connection angles to change. As the motif has been laid out, any change in the branch angle will cause the same combined amount of change in the branch-connection angles. Since the branching at each branch circle was changed by θ_i, the branch angle at each of these circles cannot change more than $\theta_i/2$, giving the equation, $\alpha_i' = \alpha_i + \frac{\theta_i}{2} d_i$ where $0 \leq d_i \leq 1$.

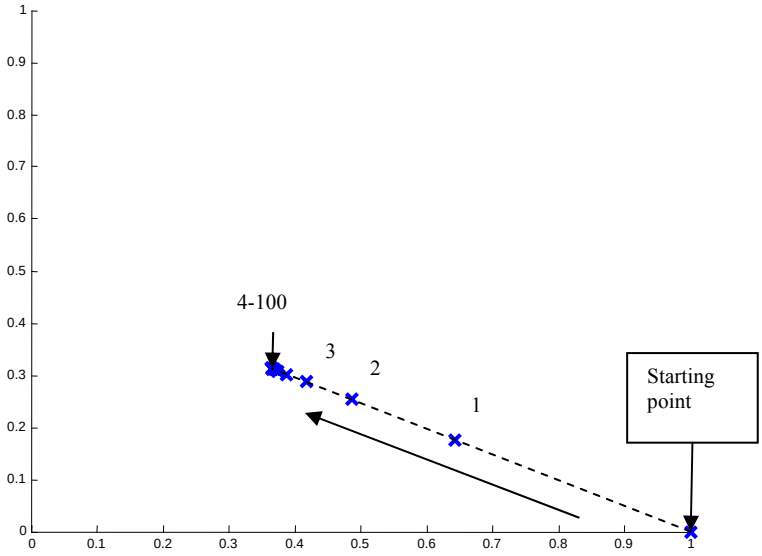

Figure 6-4: The algorithm applied to the motif 100 times.

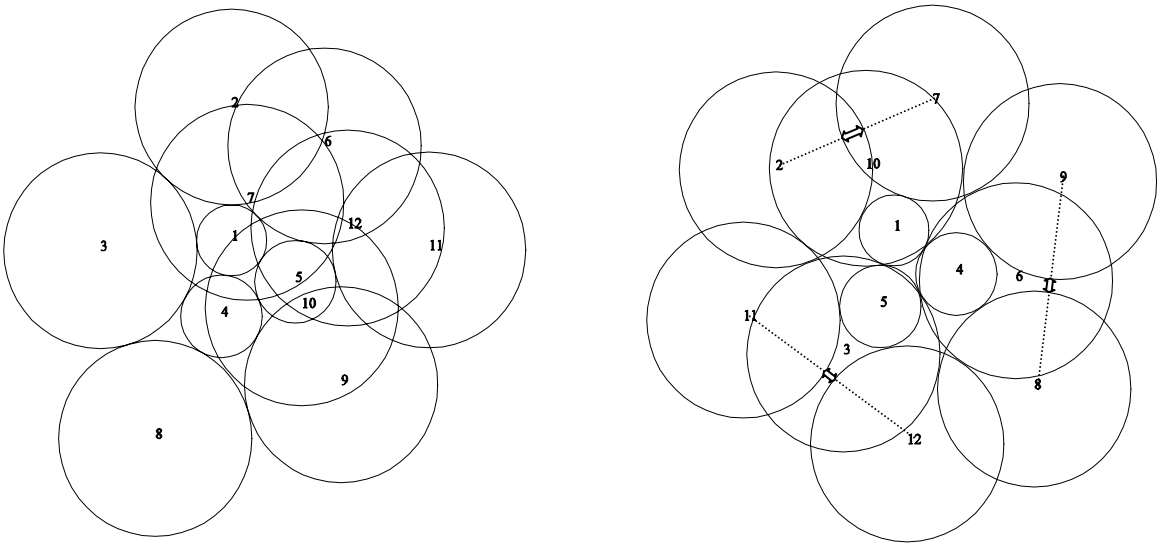

Figure 6-5: Another description of an incoherent packing, which has the location of where tangency fails moved to the non-connection circles.

The new branching was set to twice the original branch angle. So after applying the algorithm, the difference between a branch circle's branching and its branch angle is, $b_i^{'} - 2\alpha_i^{'} = 2\alpha_i - 2\alpha_i^{'} = 2\alpha_i - 2(\alpha_i + \frac{\theta_i}{2} d_i) = -\theta_i d_i$. A change in branching can only occur if one or more of the branch radii change. This implies that the partial angle sum of one or more of the branch radii will account for part of that branch circle's angle sum change.

Hence, there will be at least one new branch angle such that $\alpha_i^{'} = \alpha_i + \frac{\theta_i}{2} d_i$ where $0 \le d_i < 1$. So the new error is $E' = \left|b_1^{'} - 2\alpha_1^{'}\right| + \left|b_2^{'} - 2\alpha_2^{'}\right| + \left|b_3^{'} - 2\alpha_3^{'}\right|$, and then $E^{'} < E$. Because E is decreasing, it either goes to zero or goes to a positive limit.

The algorithm is decreasing; which implies that if E converges to a positive limit either one or two of the angle differences, $\theta_i = b_i - 2\alpha_i$, will be zero. By Lemma 2 at least two of the branch radii will change whenever the branching distribution is changed. Thus we must have at least two that converge to 0. The sum of the branching is always 2π so then $\theta_1 + \theta_2 + \theta_3 = 0$. It follows that if two of the angle differences are zero than the third will also be zero. Hence the algorithm will always find the correct branching.

Chapter 7
Geometry on a Coherent Packing

A coherent packing is a very aesthetic piece of geometry. The tri-branched coherent packing shown in Figure 7-1 is particularly pleasing. A proper exploration of all the possible relations hidden under its deceptively simple appearance would require a different work devoted entirely to this purpose. Here a couple of quick examples will be presented.

Example 1. For our first example we will refer to the coherent tri-branched packing in Figure 7-2. In a coherent tri-branched packing each connection circle is the vertex of an angle formed by its branch neighbors. If these three angles are combined with the three branch-connection angles then their sum is 2π, and they form a hexagon as in Figure 7-3.

Proof. Suppose we have a tri-branched coherent packing with branch circles $B_1, B_2,$ and B_3. Recall that if a tri-branched motif is coherent then the connection angle is equal to,

$$\underset{B_1}{\forall}{}^{1}\vec{C}^{2}\,{}^{1}\vec{C}^{3} = -\underset{B_1}{\vee}{}^{B_2}\,{}^{B_3} + \underset{B_1}{\vee}{}^{B_2}\,{}^{1}\vec{C}^{2} + \underset{B_1}{\vee}{}^{B_3}\,{}^{1}\vec{C}^{3}$$

So then the angle of the face compose by ${}^{1}\vec{\vec{C}}^{2}$, B_1 and B_2 with ${}^{1}\vec{\vec{C}}^{2}$ as the vertex is,

$$\underset{{}^{1}\vec{C}^{2}}{\vee}{}^{B_1}\,{}^{B_2} = \pi - \underset{B_1}{\vee}{}^{B_2}\,{}^{1}\vec{C}^{2} - \underset{B_2}{\vee}{}^{B_1}\,{}^{1}\vec{C}^{2}$$

Combining the angles yields,

$$\underset{B_1}{\forall}{}^{1}\vec{C}^{2}\,{}^{1}\vec{C}^{3} + \underset{B_2}{\forall}{}^{2}\vec{C}^{3}\,{}^{1}\vec{C}^{2} + \underset{B_3}{\forall}{}^{1}\vec{C}^{3}\,{}^{2}\vec{C}^{3} + \underset{{}^{1}\vec{C}^{2}}{\vee}{}^{B_1}\,{}^{B_2} + \underset{{}^{1}\vec{C}^{3}}{\vee}{}^{B_1}\,{}^{B_3} + \underset{{}^{2}\vec{C}^{3}}{\vee}{}^{B_2}\,{}^{B_3}$$

$$-\underset{B_1}{\vee}{}^{B_2}\,{}^{B_3} + \underset{B_1}{\vee}{}^{B_2}\,{}^{1}\vec{C}^{2} + \underset{B_1}{\vee}{}^{B_3}\,{}^{1}\vec{C}^{3} - \underset{B_2}{\vee}{}^{B_1}\,{}^{B_3} + \underset{B_2}{\vee}{}^{B_1}\,{}^{1}\vec{C}^{2} + \underset{B_2}{\vee}{}^{B_3}\,{}^{2}\vec{C}^{3} - \underset{B_3}{\vee}{}^{B_1}\,{}^{B_2} + \underset{B_3}{\vee}{}^{B_1}\,{}^{1}\vec{C}^{3} + \underset{B_3}{\vee}{}^{B_2}\,{}^{2}\vec{C}^{3}$$

$$+\pi - \underset{B_1}{\vee}{}^{B_2}\,{}^{1}\vec{C}^{2} - \underset{B_2}{\vee}{}^{B_1}\,{}^{1}\vec{C}^{2} + \pi - \underset{B_2}{\vee}{}^{B_3}\,{}^{2}\vec{C}^{3} - \underset{B_3}{\vee}{}^{B_2}\,{}^{2}\vec{C}^{3} + \pi - \underset{B_1}{\vee}{}^{B_3}\,{}^{1}\vec{C}^{3} - \underset{B_3}{\vee}{}^{B_1}\,{}^{1}\vec{C}^{3}$$

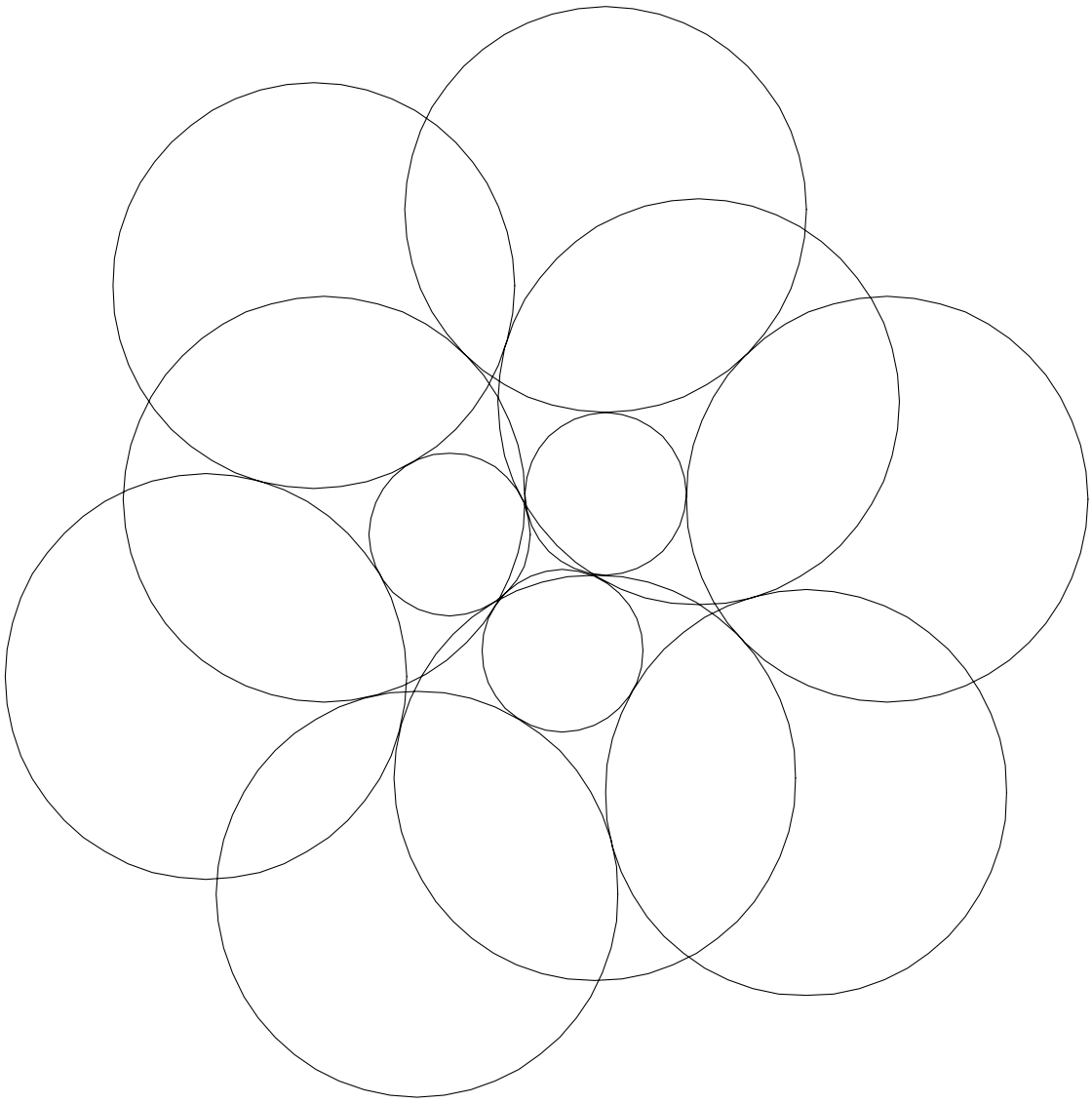

Figure 7-1: A coherent tri-branched packing.

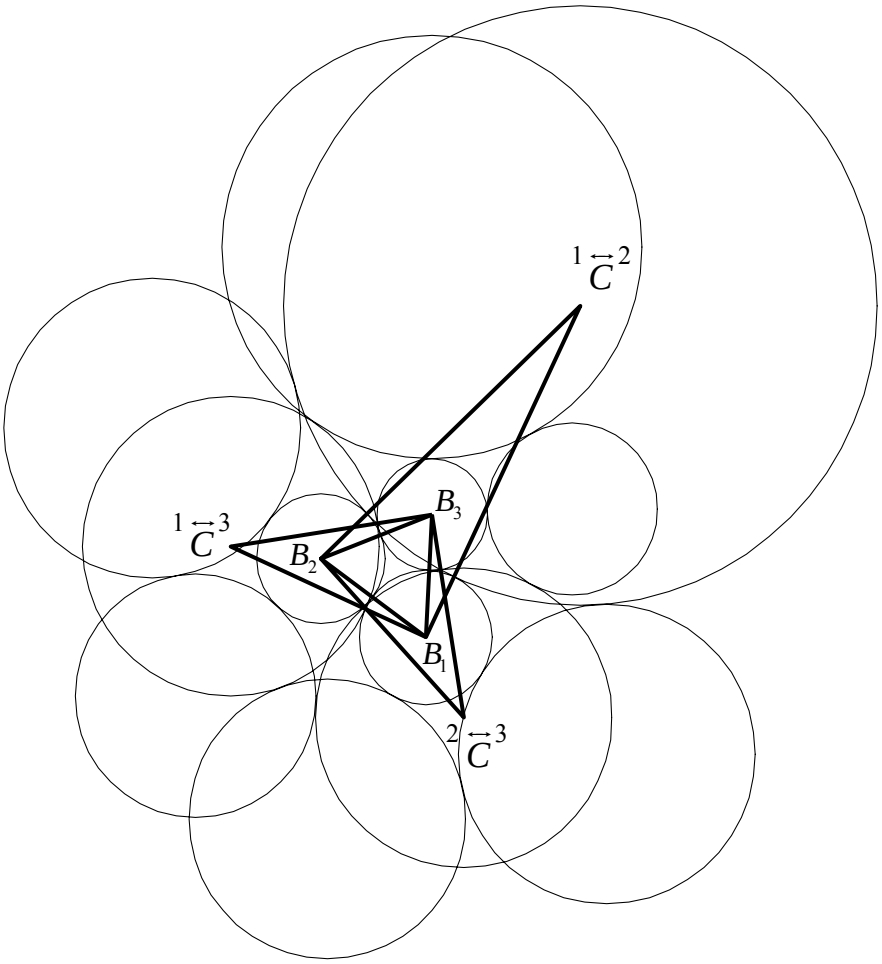

Figure 7-2: A coherent tri-branched packing rendered from the circle packing in Figure 4-1.

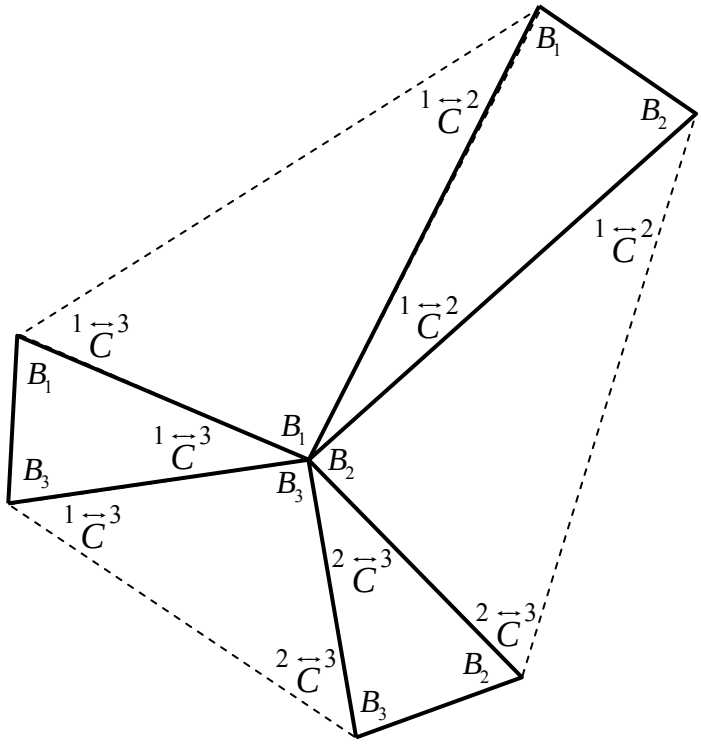

Figure 7-3: The hexagon constructed from the angles in Figure 7-2.

Grouping terms together,

$$(-\underset{B_1}{\overset{B_2}{\vee}}\overset{B_3}{} - \underset{B_2}{\overset{B_1}{\vee}}\overset{B_3}{} - \underset{B_3}{\overset{B_1}{\vee}}\overset{B_2}{}) + (\underset{B_1}{\overset{B_2}{\vee}}\overset{{}^1\vec{C}^2}{} - \underset{B_1}{\overset{B_2}{\vee}}\overset{{}^1\vec{C}^2}{}) + (\underset{B_1}{\overset{B_3}{\vee}}\overset{{}^1\vec{C}^3}{} - \underset{B_1}{\overset{B_3}{\vee}}\overset{{}^1\vec{C}^3}{}) + (\underset{B_2}{\overset{B_1}{\vee}}\overset{{}^1\vec{C}^2}{} - \underset{B_2}{\overset{B_1}{\vee}}\overset{{}^1\vec{C}^2}{})$$
$$+(\underset{B_2}{\overset{B_3}{\vee}}\overset{{}^2\vec{C}^3}{} - \underset{B_2}{\overset{B_3}{\vee}}\overset{{}^2\vec{C}^3}{}) + (\underset{B_3}{\overset{B_1}{\vee}}\overset{{}^1\vec{C}^3}{} - \underset{B_3}{\overset{B_1}{\vee}}\overset{{}^1\vec{C}^3}{}) + (\underset{B_3}{\overset{B_2}{\vee}}\overset{{}^2\vec{C}^3}{} - \underset{B_3}{\overset{B_2}{\vee}}\overset{{}^2\vec{C}^3}{}) + 3\pi = -\pi + 3\pi = 2\pi$$

The sides of the triangles will match together as in the picture since their sides are of equal length. If the circles in the motif are all laid out so that they are tangent then the equation for the connection equation will hold and the converse is also true.

Example 2. Figure 7-4 is another similar result that can be constructed with a coherent tri-branched packing. The same triangles used in Figure 7-3 are used here, only they have been placed repeatedly and in a slightly different order. The proof is similar to the one used in Example 2 and is omitted here.

In the hexagon pictured in Figure 7-3, the sides opposite the connection angles can be extended until they intersect. The triangle formed by connecting these intersections is similar to the triangle formed by connecting the vertices of the connection circles (the *connection triangle*) the hexagon was derived from. This is best demonstrated with Figure 7-5.

This is a picture of the same coherent packing used to build the hexagon in Figure 7-3. Just the complex of the branch circles and connection circles is shown with the connection triangle highlighted. A series of parabolic shifts of each of the triangles using the angles $\underset{{}^1\vec{C}^2}{\overset{B_2}{\vee}}\overset{B_1}{}$, $\underset{{}^1\vec{C}^3}{\overset{B_3}{\vee}}\overset{B_1}{}$, and $\underset{{}^2\vec{C}^3}{\overset{B_3}{\vee}}\overset{B_2}{}$ gives the hexagon.

The complex shown will have matching vertices for circles that are drawn tangent (all circles not just the branch and connection circles) if and only the packing is coherent. So this statement could be used as a slicker proof of Example 1. It would not be surprising to discover that a condition for coherency is dependent on the connection triangle. Experiments have suggested that the connection triangle prior to

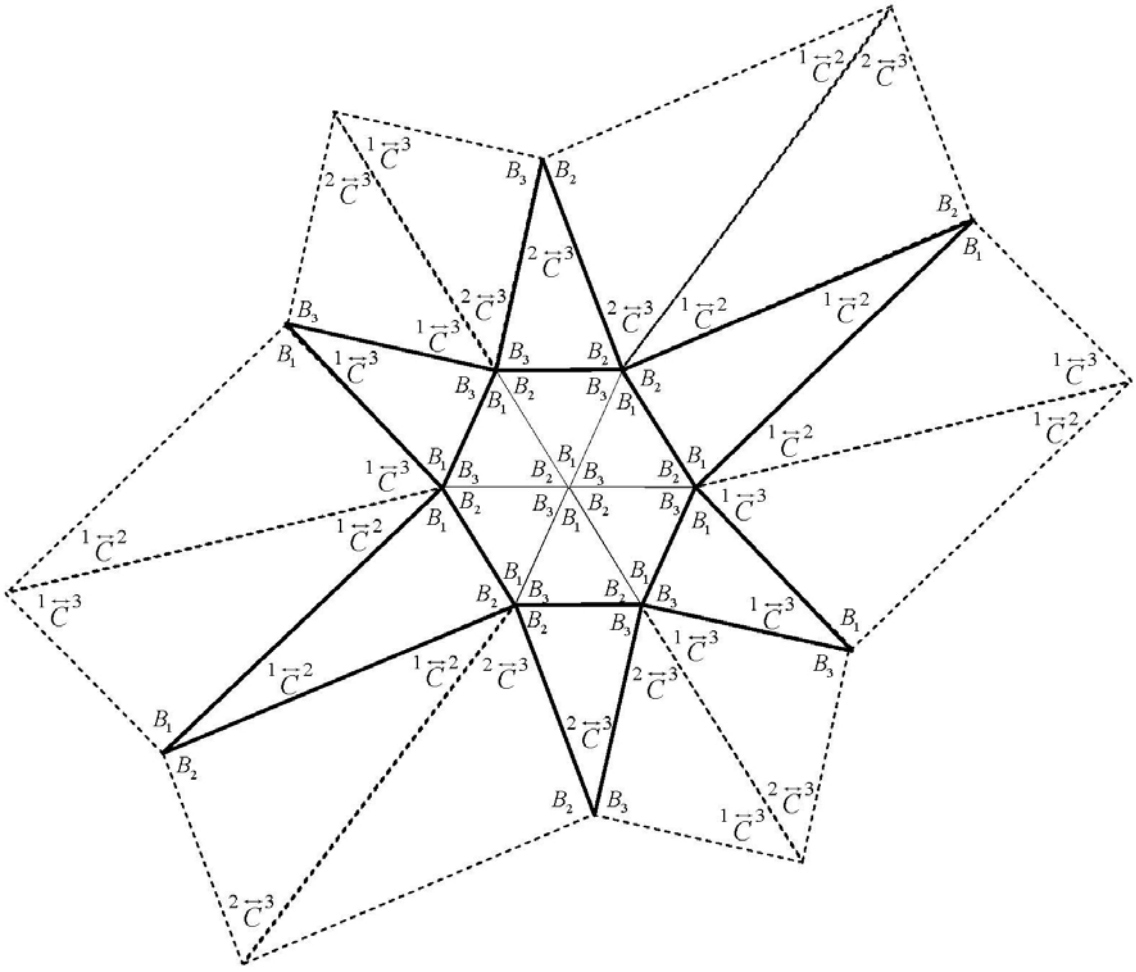

Figure 7-4: A geometric shape render from the coherent packing in Figure 7-2.

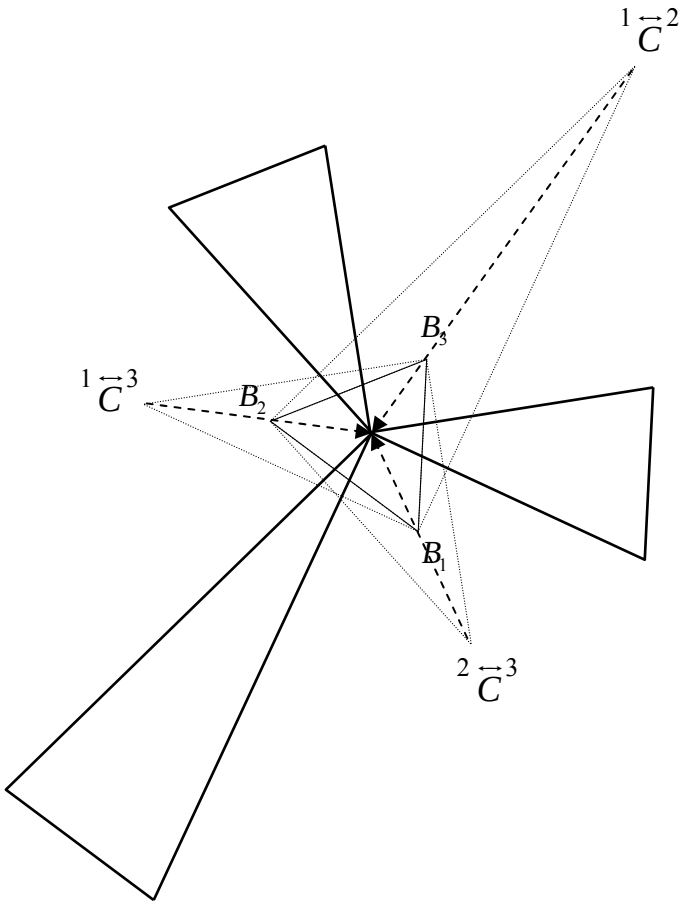

Figure 7-5: The shifts that can used to construct the hexagon in Figure 7-3

branching is more influential on a coherent packing's structure than the radii of the border circles.

Although an exact equation for computing circle packings does not exist, one might for branched packings. It may even be possible to make Euclidean constructions of tri-branched packings in special situations or even in the general case. Regardless of the circumstances, it is certain that there is much left to explore.

Chapter 8
Closing Thoughts

Things have wrapped up rather nicely, but there is still much work that needs to be done. Experiments strongly suggest that all of the results shown here could in fact be generalized to non-simple circle packings. Furthermore, experiments have suggested that all of these results would hold without assuming mutual tangency for the branch circles. If true, it would be an interesting result since this property was key to proving uniqueness.

This would be of value since the question of using tri-branched packings in application to discrete functions would be closed. On this subject (it was after all the original motivation for these problems) the use of a fourth branch circle seems as though it would provide the needed flexibility. Using three branch circles has the strength of a triangle, but using four is like a bookcase without any shelves that flops over.

This investigation was restricted to the plane. A study of fractured branched packings on hyperbolic or even spherical geometry could be very interesting. Most interesting to the author, however, is the possibility of a whole new breed of geometry problems. Stare for a few minutes at a coherent tri-branched packing and a myriad of relations seem ready to leap out. The optimism expressed here for the future of fractured branched packings may be nothing more than wishful thinking kindled by the recent entertainment of these problems, but the author feels confident that there is much more to be found beyond the horizon.

Bibliography

Bibliography

[1] Kenneth Stephenson, Circle Packing: A Mathematical Tale. *Notes of the AMS,* **50** (2003), no. 11, 1379-1380.

[2] _____ , Circle Packing: A Mathematical Tale. *Notes of the AMS,* **50** (2003), no. 11, 1379-1380.

[3] Chuck Collins and Kenneth Stephenson, A Circle Packing Algorithm, *Computational Geometry: Theory and Applications,* **25** (2003), 233-256.

[4] Kenneth Stephenson, '6.2 The Monodromy Theorem', notes from a seminar in analysis (2001), 5-8. (to appear in a book on Circle Packing by 2005).

[5] _____ , '6.2 The Monodromy Theorem', notes from a seminar in analysis (2001), 5-8. (to appear in a book on Circle Packing by 2005).

Vita

James Russell Ashe was born December 30, 1975. In 1994 he graduated from Greeneville High School in Greeneville Tennessee. He attended and graduated from East Tennessee State University in 1999 with a Bachelors of Science in History with a minor in art. In 2004 he completed the requirements for a Masters of Science in Mathematics at the University of Tennessee.